FINAL PUBLISHABLE REPORT

Grant Agreement number	17FUN08
Project short name	TOPS
Project full title	Metrology for topological spin structures

<table>
<tr><td colspan="2">Project start date and duration:</td><td>01 June 2018, 42 months</td></tr>
<tr><td colspan="3">Coordinator: Mark Bieler, PTB   Tel: +49-531-592-2540   E-mail: mark.bieler@ptb.de
Project website address: https://www.ptb.de/empir2018/tops</td></tr>
<tr><td>Internal Funded Partners:
1 PTB, Germany
2 INRIM, Italy
3 NPL, United Kingdom</td><td>External Funded Partners:
4 Singulus, Germany
5 TUM, Germany
6 ULE, United Kingdom
7 UNIPG, Italy</td><td>Unfunded Partners:
-</td></tr>
<tr><td colspan="3">RMG1: INRIM, Italy (Employing organisation); PTB, Germany (Guestworking organisation)</td></tr>
</table>

TABLE OF CONTENTS

1 Overview

In recent years, topology (the study of the properties of geometric configurations which are unaltered by certain elastic transformations such as a stretching, bending or twisting) has emerged as a fascinating phenomenon in solid state research from both fundamental and applied perspectives. This is particularly the case for certain magnetisation configurations, where the topology protects the spatial magnetisation or spin arrangement. Due to their unique properties, such topologically-protected spin structures (TSS) have the potential to revolutionise the Information and Communications Technology sector. This project has supported fundamental research in this active field by developing metrological tools and methods for the characterisation of TSS. This includes accurate measurements of the Dzyaloshinskii-Moriya interaction (DMI) constant, spatially-resolved methods for the identification and manipulation of multiple and individual TSS, and reliable concepts for the investigation of dynamical properties of TSS. With these project results, the scientific community has now more information as well as better tools and techniques at hand, which will be helpful for the possible realisation of microwave and magnonics related applications based on TSS. Moreover, the DMI-measurement comparison has created awareness in the scientific community of the reliability and unreliability of measurement results.

2 Need

Fundamental research in the field of spintronics has led both to the recognition of scientific merits at the highest level and to extremely fast development of a huge market sector dealing with mass production of consumer and industrial electronics, such as hard disk storage devices and sensors for mobile phones and cars. The search for new materials featuring room temperature operation, ultralow power consumption, full electrical control, and scalability continues apace. Several years ago, the study of spin structures with a certain topologically-protected spin arrangement, has moved into worldwide focus. Despite intensive research on TSS (such as *chiral domain walls* which are boundaries between regions of uniform magnetisation with a certain gradual rotation of the magnetisation or *skyrmions,* which are vortex-like spin arrangements with diameters typically ranging between several nm to several 100 nm), there have been several high-level requirements in this field connecting basic research, metrology, and ability to exploit these structures in novel devices that needed to be addressed:

- The quest for new materials and systems with stable TSS requires a precise understanding and knowledge of relevant material parameters such as the Dzyaloshinskii-Moriya interaction (DMI) constant. However, validated metrology tools for these parameters did not exist.

- Due to their nanoscale size, it is difficult to experimentally probe some types of TSS. Therefore, validated measurement methods were needed enabling the identification and manipulation of multiple and individual TSS.

- Reliable concepts for the investigation of current- and field-induced dynamics of TSS at GHz and THz frequencies had to be developed. In addition, experimental high-risk-high-gain research was required to verify whether TSS enable the realisation of novel quantum standards.

- Additional research on TSS required the fabrication of TSS with reproducible topological characteristics. Micromagnetic simulations and analytical tools were required to validate experimental results and to reliably predict novel material properties.

3 Objectives

The overall objective of this project was to develop and establish metrological and scientific tools for the characterisation of TSS. This work was expected to significantly contribute to the development of new magnetic storage, spin-logic, and microwave devices in the future well as new quantum standards.

The specific objectives of this project were:

1. To develop and validate metrology tools and methods for reliable determination of key material parameters of TSS, i.e., the Dzyaloshinskii-Moriya interaction (DMI) constant.

2. To develop, compare and validate measurement techniques capable of unambiguously identifying and manipulating specific nanometre-scale TSS, such as domain walls, bubbles, and skyrmions in different magnetic materials. These methods would be applicable to both multiple and individual TSS.

3. To develop methods for the investigation and analysis of novel dynamical and quantisation effects in TSS. This work would capture the dynamics of TSS at GHz and THz frequencies and explore whether TSS might serve as quantum standards at room temperature and low magnetic fields.

4. To provide protocols for the reproducible growth of materials for experiments on TSS and reliable micromagnetic simulations and analytical tools for the modelling of TSS. The simulations would allow for a comparison with and an interpretation of experimental results.

5. To implement a research network on TSS in Europe with complementary infrastructure. To develop guidelines for accurate characterisation of TSS and to implement new measurement services on the DMI constant.

4 Results

The results achieved within this project will be discussed separately for each objective.

4.1 Reliable determination of key material parameters of TSS (objective 1)

4.1.1. Literature review

Considering the Web of Science database, about 1500 articles on the topic of DMI have been published since 2000, reaching the remarkable record of 7000 citations in 2018 only. In particular, the interfacial DMI, stabilizing skyrmions and chiral DWs in thin film systems, is especially interesting from applicative point of view, attaining extremely efficient domain wall motion for future spintronic applications as sensors or memories. It occurs in systems composed of a heavy metal (HM) layer and an ultrathin ferromagnetic (FM) film with perpendicular magnetic anisotropy (PMA) (e.g., FM: Co, CoFeB; HM: Pt, Ta, Ir, W). A classification of HM/FM material combinations for their DMI strength, described by the related energy coefficient D, is therefore highly desirable, but requires the accurate measurement of the magnitude and sign of the DMI. Nevertheless, a detailed literature review was not yet available and an established and reliable method to measure DMI is still lacking. We therefore published a literature review on measuring the interfacial DMI. The most commonly used experimental techniques that in recent years have been employed can be broadly divided into three categories:

a) Domain wall methods, where D is extracted by either measuring the domain wall velocity or energy as a function of an in-plane magnetic field, or by measuring domain wall spacing in stripe domain phases, or by directly measuring the domain wall internal structure;

b) Spin wave methods, where D is extracted by measuring the non-reciprocity of propagating spin waves, owing to the presence of DMI, in in-plane magnetised films;

c) Spin-orbit torque methods, where D is extracted by measuring the field shift of the out-of-plane hysteresis loop under an in-plane magnetic field.

We analysed the advantages and limitations of all methods and try to give general rules for their applicability. The two most popular methods employed by the community are the asymmetric bubble expansion method using the magneto-optic Kerr effect (MOKE) and the determination of spin wave non-reciprocity exploiting Brillouin light scattering (BLS). While general trends for classifying materials according to their DMI strength could be established (see Fig. 1), disagreement in the attempt of reliably quantifying DMI by measuring D, especially for small DMI (D < 0.5 mJ/m2). Not only different measuring techniques deliver contradictory values for D, but results are even controversary when the same method on nominally identical stacks is employed. The discrepancies observed are well above the measurement uncertainty for a single technique. One origin for the discrepancies is the fact that the DMI is extremely sensitive to the interface quality, and therefore to differences in sample preparation or presence of defects, impurities, oxidation, etc.. Nominally same samples may produce D values varying 1-10 times. Therefore, studies performed with different techniques on the same sample are very valueable, but still rare (< 10 papers are found in literature).

For further information on this topic contact Michaela Kuepferling (m.kuepferling@inrim.it) and see https://doi.org/10.48550/arXiv.2009.11830.

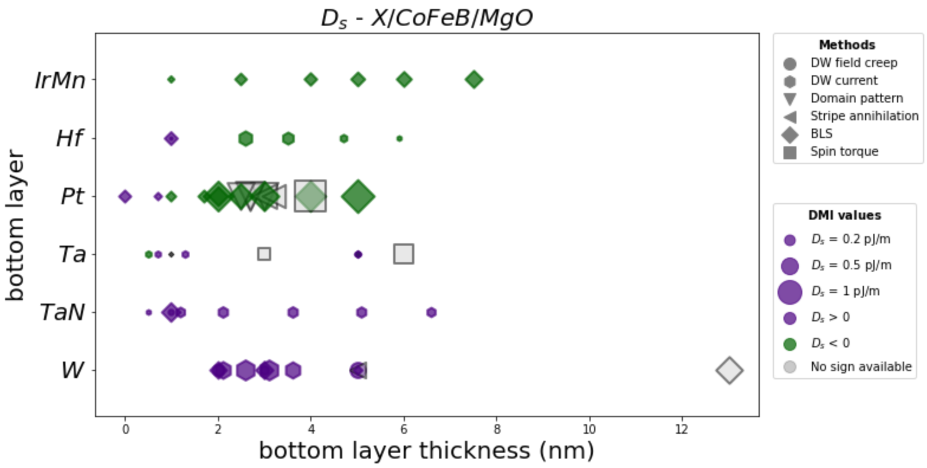

Fig. 1: Literature data for X/CoFeB/MgO of the DMI constant D_S=D.t, t the FM thickness. The bottom layers X = (IrMn, Hf, Pt, Ta, TaN, W) are the most popular in the literature. The shapes of the symbols refer to different experimental methods, while their size and color reflect the amplitude and the sign of D_S, respectively, as specified in the legends on the right. Data for methods not able to determine the sign of D_S (i.e, domain pattern, stripe annihilation and spin torque) are in grey. Most of the data (> 70%) are for a MgO thickness of 2 nm, with nearly 20% for 1 nm.

4.1.2. Round robin comparison

An accurate comparison within an international Round Robin was undertaken within the TOPS project with the aim to clarify the origin of the discrepancies shown in the literature review. The comparison was performed by the two of the most popular techniques, asymmetric bubble expansion method using the magneto-optic Kerr effect (MOKE) and the determination of spin wave non-reciprocity exploiting Brillouin light scattering (BLS). We analysed in detail the measurement process and evaluation of D, in order to provide recommendations to the community for the reliable and accurate measurement of the DMI. We find that the MOKE method can be applied to a wide variety of heterostructures with magnetic bubble domains, but its applicability depends strongly on the interface quality and the applied theoretical model for the evaluation.

We compared different models and find that the ones based on the standard creep hypothesis are not able to reproduce the DW velocity profile when the DW roughness is high. For example, in multilayers with several repetitions the interface quality may deteriorate and we observed rough DWs or transitions to maze domains. Our results demonstrate that the DW roughness and the interface roughness of the sample layers are correlated. The rougher the bubble DW, the more difficult is it to identify the DW velocity and its minimum in order to evaluate D. The automatized determination of the DW velocity by using a software package (published at GitHub) may be a future tool for a more reliable analysis. Concerning the identification of the minimum velocity by models, samples characterized by a lower DW roughness can be modelled by the standard creep model, while the arbitrary angle propagation model provides insights on the presence of magnetic effects from neighbouring bubbles. This implies that the bubble expansion proceeds initially very slowly due the high density of pinning sites. Samples with induced defects by irradiation instead show different behaviour. Bubble DWs are slightly rough, but well defined and the velocity curves are well determined. There is no flat region but a change of slope well described by the dispersive stiffness model. The D value is increasing with increasing irradiation. As a result we give guidance on how to obtain reliable results for the DMI value with this popular method and indicate the actual measurement uncertainty.

The BLS method appears to be more versatile, having a more straightforward evaluation of the DMI and being less sensitive to defects and inhomogeneities of the sample. However, we find in some cases large differences in the measured value, with BLS resulting in a higher DMI (see Fig.2). In the literature, it was shown that for certain samples using more sophisticated models for the evaluation of the MOKE data a better agreement between the techniques can be obtained. However, it remains to be investigated in the future if there are intrinsic differences between the techniques.

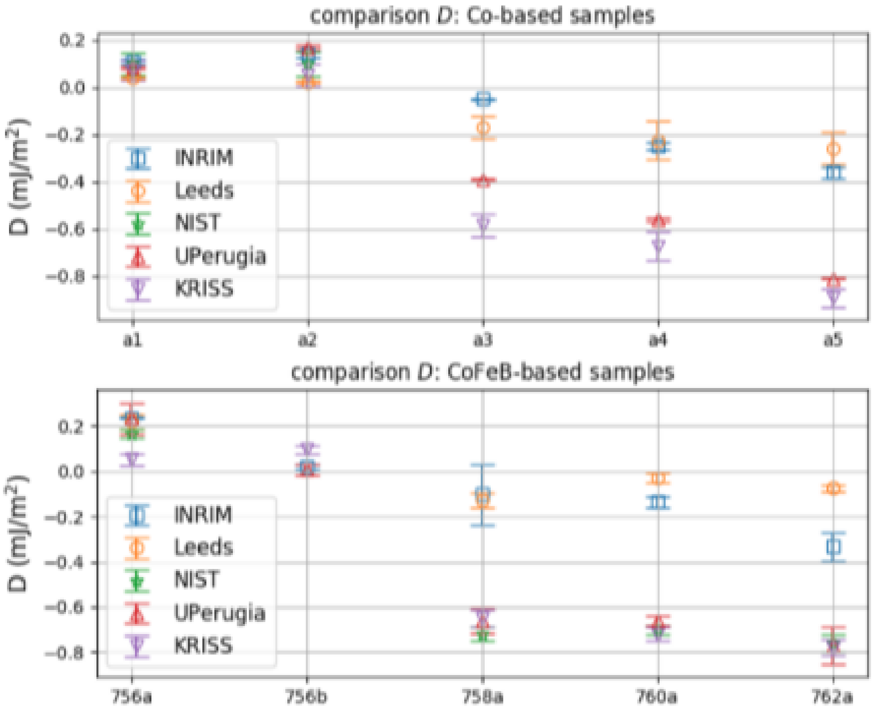

Fig. 2: D measured by MOKE at INRIM and Univ.Leeds and by BLS at NIST, Univ.Perugia and KRISS. Upper panel: Ta(5)/Pt(3)/Co(0.8) with top layers a1 Pt(3)/Ta(3), a2 Pt(1)/Ta(3), a3 Ir(3)/Ta(3), a4 Ir(1)/Ta(3), a5 Ta(3). Lower panel: W(5)/$Fe_{60}Co_{20}B_{20}$(0.6)/ MgO(2)/Ta(5): 756a (annealed at 400°C) and 756b (as grown); Pt(3.4)/$Co_{60}Fe_{20}B_{20}$(0.8)/MgO (1.4)/Ta(5) at different sputter power: 758a (200W), 760a (700W), 762a (1200W). All nominal thicknesses in nm.

For further information on this topic contact Michaela Kuepferling (m.kuepferling@inrim.it) and see https://doi.org/10.48550/arXiv.2201.04925.

4.1.3. Good practice guide

In order to provide recommendations on how to reliably measure the DMI value, we prepared a good practice guide on the measurement of the interfacial Dzyaloshinskii-Moriya interaction (DMI) in heavy metal (HM)/ ferromagnet (FM) bi- or multilayers by Brillouin light scattering (BLS) (the principle of the measurement of D by BLS is shown in Fig. 3). It emphasizes key-points for the reliable determination of the D constant, describing the strength of the DMI, and gives recommendations on how to improve the measurement uncertainty. With respect to domain wall (DW) based methods (such as the asymmetric bubble expansion method), spin wave methods have the advantage of a more straightforward evaluation of the D constant, without the need for choosing the correct model. Furthermore, they seem to be less sensitive to defects and inhomogeneities of the sample. Among the SW methods, BLS is currently the most “handy” method, as it does not require any external spinwave transduction or any kind of patterning, contrary to time-resolved magneto-optical Kerr effect and propagating spin wave spectroscopy. The frequency shift in the spectra, caused by DMI, can be measured with high accuracy. The uncertainty in the frequency shift is low and difficulties in the measurement occur mainly in presence of high damping, where the spin wave signal can be small and affected by larger errors (due to broad peaks in the BLS spectra). The uncertainty of D is therefore mainly determined by the uncertainty of the parameters entering the model that evaluates D from the frequency shift. These are the gyromagnetic ratio, the saturation magnetization and the wavevector. The good practice guide shows the potential of BLS to be used as a standard technique for measurement services provided to the scientific or industrial community. The good practice guide will be soon published open access at https://zenodo.org/communities/inrim.

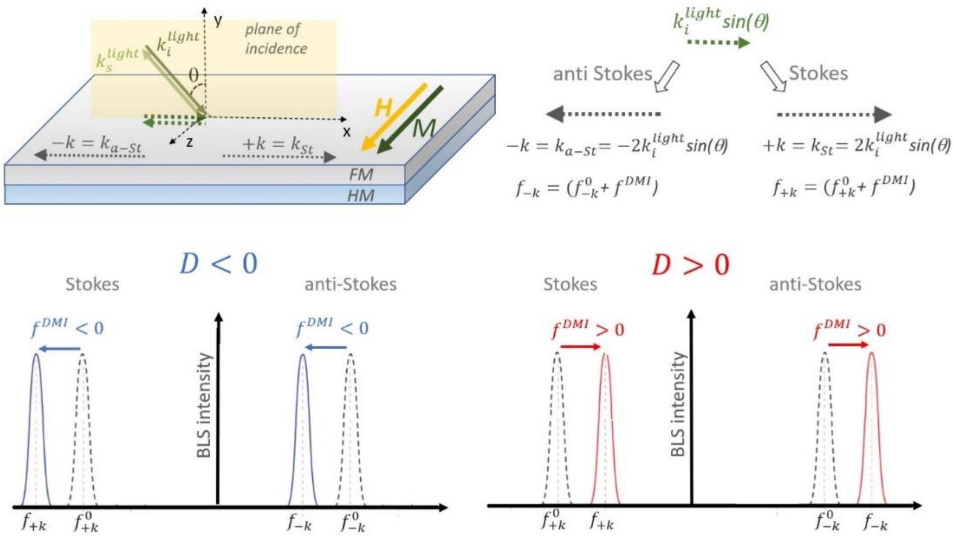

Fig. 3: Schematic diagram of the BLS measurement. The frequency of the inelastically scattered light is measured by a interferometer. The scattering results in two frequency peaks in the spectrum, shifted with respect to the incident beam (Stokes and anti-Stokes). Both peaks are shifted in presence of DMI, the frequency shift is proportional to the DMI strength while the sign is observed as blue or red shift.

For further information on this topic contact Michaela Kuepferling (m.kuepferling@inrim.it), Giovanni Carlotti (giovanni.carlotti@unipg.it).

4.1.4. Key Outputs and Conclusions

Different methods have been proposed to evaluate the interfacial Dzyaloshinskii-Moriya interaction (DMI). The two most popular methods employed by the scientific community are the asymmetric bubble expansion method using the magneto-optic Kerr effect (MOKE) and the determination of spin wave non-reciprocity exploiting Brillouin light scattering (BLS).

In a worldwide first international round robin comparison, the project partners and collaborators compared these two methods and focused, in particular, on the MOKE method, which was envisioned as a possible candidate for a measurement service. Since the evaluation of the DMI constant from the MOKE measurement is an ongoing discussion in the community, the most promising theoretical models applied to a range of different magnetic multilayers with perpendicular magnetic anisotropy (PMA) have been investigated for the extraction of the DMI constant using measured MOKE data. The asymmetric bubble expansion method can be applied to a wide variety of heterostructures with magnetic bubble domains. However, its applicability depends strongly on the interface quality. It was found that models based on the standard creep hypothesis are not able to reproduce the domain wall (DW) velocity profile when the DW roughness is high. The project results demonstrate that the DW roughness and the interface roughness of the sample layers are correlated. The rougher the bubble DW, the more difficult is it to identify the DW velocity and its minimum in order to evaluate the DMI constant.

The automatized determination of the DW velocity by using a software package, which was published at GitHub, may be a future tool for a more reliable analysis. Concerning the identification of the minimum velocity by models, samples characterized by a lower DW roughness can be modelled by the standard creep model, while the arbitrary angle propagation model provides insights on the presence of magnetic effects from neighbouring bubbles. Samples with induced defects by irradiation instead show different behaviour. The DMI value is increasing with increasing irradiation. As a result of the investigations, guidance was given on how to obtain reliable results for the DMI value with this popular method including corresponding measurement uncertainties. A comparison of the results with BLS measurements on the same samples showed that the BLS approach often results in higher measured values of DMI. This fact is topic of ongoing research. A corresponding paper has been submitted to a peer reviewed journal and uploaded to the arXiv (https://arxiv.org/abs/2201.04925).

Based on these results, this objective was successfully achieved.

4.2 Unambiguous identification and manipulation of specific nanometre-scale TSS (objective 2)

4.2.1. Radial dependent stray field signature of chiral magnetic skyrmions

We have used qMFM to analyse the radial dependent phase response of skyrmions in chiral Co/Ru/Pt magnetic multilayers. To achieve this, we used a nucleation protocol that was developed as part of the work undertaken, where, we have used thermoelectric measurements to characterise the presence of skyrmions in the device. In this work using the developed protocol, we studied a small set of skyrmions (six in total Fig. 4(a)) investigating the size dependence of the measure qMFM signal. Size dependent control was achieved using in situ electromagnet to apply a magnetic field within the experimental system. A combination of qMFM deconvolution processes and image analysis allowed us to investigate any size dependence on the experimentally measured signal. Our experimental results showed that there is a distinct trend in the measured phase signal and the skyrmion radial dependence with applied magnetic field. To understand the experimentally measure trend, a simple model that treats the skyrmion size r and domain wall w was developed. In this model, both r and w are treated as independent parameters which we can easily explore the expected phase response space, Fig. 4(b). This approach offers a simple method to determine r and w which could be more adaptable to that of using numerical models.

We also explore the spatial frequency spectra for the calculated skyrmion stray magnetic field distributions to understand the experimentally observed trend. We find that the trend can be described as resulting from a trade-off of the evolution of the spatial frequencies of the skyrmion stray field during the convolution with the TTF. Ultimately, this modifies the force interaction leading to a radial dependant phase response.

By comparing the experimental results with the simple model, we show that our skyrmions are Neél type. We find that he spins rotate away from the core, as expected for our multilayer system. We also show that the domain wall transition width $w \lesssim 16\,nm$, red dashed line Fig. 4(b). Interestingly, we can also estimate the smallest skyrmion radius that should be experimentally measurable for the ambient conditions used. For our experiment this was found to be $24\,nm$.

The results obtained emphasise how qMFM can be used to investigate the underlying spin structure of technologically relevant skyrmions which can be used to validate results from numerical or micromagnetic simulations.

For further information on this topic contact Craig Barton (craig.barton@npl.uk).

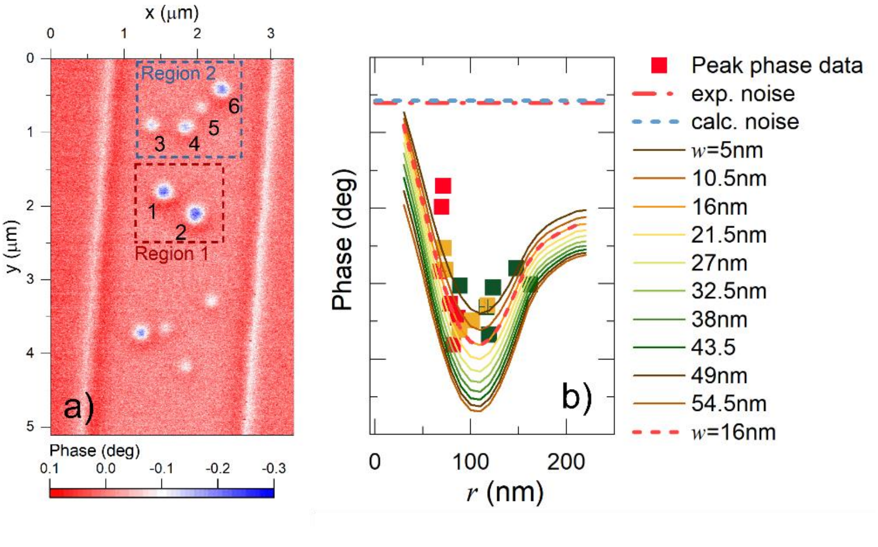

Fig. 4: (a) Overview micrograph showing the six skyrmions studied by qMFM. (b) Comparison of the maximum skyrmion MFM response with radius r. The experimental data (square symbols) are shown with calculated phase response (solid lines) for the different values of w used in the calculations.

4.2.2. A Ti/Pt/Co Multilayer Stack for Transfer Function Based Magnetic Force Microscopy Calibrations

Magnetic force microscopy (MFM) is a widespread technique for imaging magnetic structures with a resolution of some 10 nanometers. MFM can be calibrated to obtain quantitative (qMFM) spatially resolved magnetization data in units of A/m by determining the calibrated point spread function of the instrument, its instrument calibration function (ICF), from a measurement of a well-known reference sample. Beyond quantifying the MFM data, a deconvolution of the MFM image data with the ICF also corrects the smearing caused by the finite width of the MFM tip stray field distribution. However, the quality of the calibration depends critically on the calculability of the magnetization distribution of the reference sample.

Part of the work explored how a Ti/Pt/Co multilayer stack can be used as a suitable reference material. A precise control of the fabrication process, combined with a characterization of the sample micromagnetic parameters, allows reliable calculation of the sample's magnetic stray field proven by a very good agreement between micromagnetic simulations and qMFM measurements. The quality of the calibration by the proposed sample is cross compared by using a well-known Pt/Co reference sample. Furthermore, the characteristic structure sizes detectable by the MFM after calibration with both Ti/Pt/Co and Pt/Co reference samples were calculated and compared, see Fig. 5.

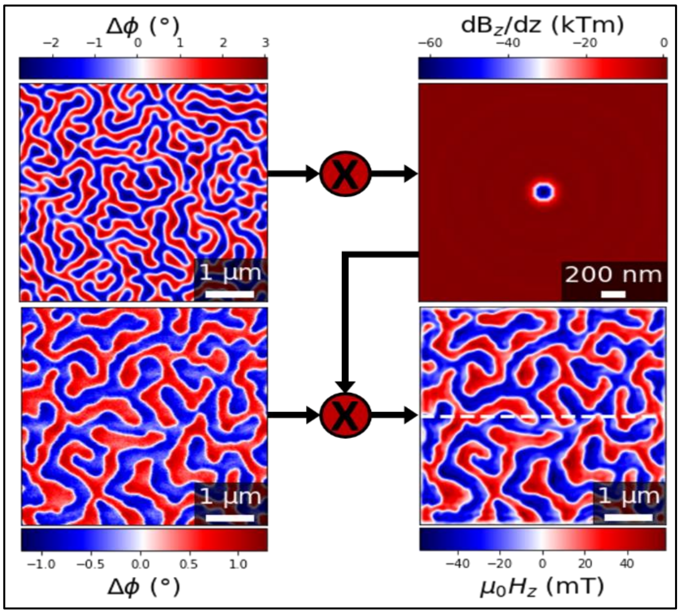

Fig. 5: Quantitative MFM measurement of Ti/Pt/Co stack. The tip transfer function (TTF) is deconvolved by using a well-known Pt/Co multilayer reference sample. The TTF is used to deconvolve the 2D stray field map from the raw MFM phase shift data of the Ti/Pt/Co sample.

For further information on this topic contact Baha Sakar (baha.sakar@ptb.de) and see https://doi.org/10.3390/magnetochemistry7060078.

4.2.3 Spin structure relation to phase contrast imaging of isolated magnetic Bloch and Néel skyrmions

Lorentz Transmission electron microscopy (LTEM) is a wide spread tool for the investigation of the local magnetization with a spatial resolution down to a few tens of nanometres. However, when investigating the local spin structure of nanometric objects such as skyrmions, the exact identification of the skyrmion size has so far not been in the focus of research teams. In particular, the most convenient and straight forward technique to observe magnetic skymions by LTEM is Fresnel imaging which is an under- or overfocus technique and thus the determination of the exact sykrmion size is challenging. Using numerical calculations, this work performed by researchers at the Technical University Munich and the University of Regensburg relates the phase contrast in an LTEM to the actual magnetization profile of an isolated Néel or Bloch skyrmion, the two most common skyrmion types. Within the framework of the used skyrmion model, the results are independent of skyrmion size and wall width and scale with sample thickness for purely magnetic specimens. Simple rules are provided to extract the actual skyrmion configuration of pure Bloch or Néel skyrmions without the need of simulations. Furthermore, first differential phase contrast (DPC) measurements on Néel skyrmions that meet experimental expectations have been presented and showcase the described principles. The work is relevant for material sciences where it enables the engineering of skyrmion profiles via convenient characterization.

For further information on this topic contact Christian Back (christian.back@tum.de) and see https://arxiv.org/abs/2002.1246.

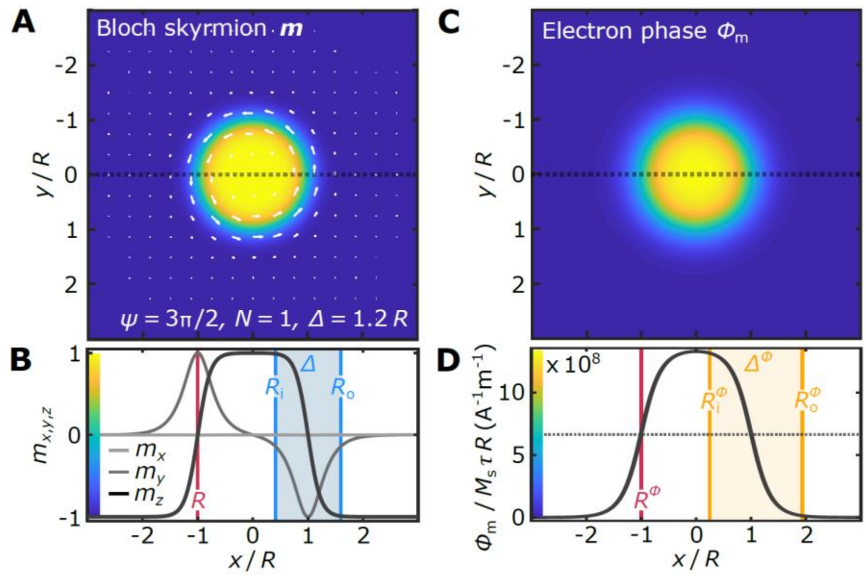

Fig. 6: (A) Example Bloch skyrmion spin structure (simulation) with indicated structural parameters. The white arrows represent the in-plane magnetization components. Coloring maps the *mz* component as indicated at the *y*-axis of (B). (B) Line profile of the components of *m* along the dotted line in A. (C) Calculated 2D electron phase of the skyrmion in (A). Coloring represents the normalized phase value as indicated at the *y*-axis of (D). (D) Line profile of the normalized electron phase along

4.2.4 Manipulation of magnetic skyrmion density in continuous Ir/Co/Pt multilayers

Logic devices based on nano-magnetism show the capability to couple ultrafast reversal of the magnetic state (or bit) with a non-volatile nature due to high thermal stability. Spintronic (awarded Nobel prize in physics 2007) storage or logic based on magnetic skyrmions are anticipated to be more efficient and to have a higher storage capacities. In fact, the small size of skyrmions allow for a significant reduction of the spacing between the bits and improves the ratio between the information flowing and the current density employed for the motion. The skyrmion topology, characterized by an integer whirling number, makes them particularly robust to the external environment and notably defects. Specifically, a multi-bit storage device using skyrmions as information carriers (bits), where the state of the device is modulated by an electric current that shifts the skyrmions in and out of the device. Such a behaviour, in which the state of the system (“weight”) can be dynamically adapted to the environment, is analogous to a biological synapse and their synaptic plasticity. This also opens a way for utilising such devices in novel applications, such as skyrmion-based artificial synapses and neuron type devices in low-power neuromorphic computing, or brain-inspired architectures for deep machine learning applications.

Part of the work that has resulted from our work involved understanding how the layered structure in a magnetic multilayer can be used to tailor magnetic skyrmions. In this work, we show that magnetic skyrmions can be stabilized at room temperature in continuous $[Ir/Co/Pt]_5$ multilayers on SiO_2/Si substrate without prior application of electric current or magnetic field, see Fig. 7. While decreasing the Co thickness, tuning of the magnetic anisotropy gives rise to a transition from worm-like domain patterns to long and separate stripes. The skyrmions are clearly imaged in both states using Magnetic Force Microscopy. The density of skyrmions can be significantly enhanced after applying the “in-plane field procedure”. In addition, we have investigated the phase diagram of a sample deposited in the same run, but onto a SiN_x membrane using Lorentz transmission electron microscopy. Interestingly, this sample shows a different behaviour as function of magnetic field hinting to the influence of strain on the phase diagram of skyrmions in thin film multilayers. Our results provide means to manipulate magnetic skyrmion density, further allowing for optimized engineering of skyrmion-based devices.

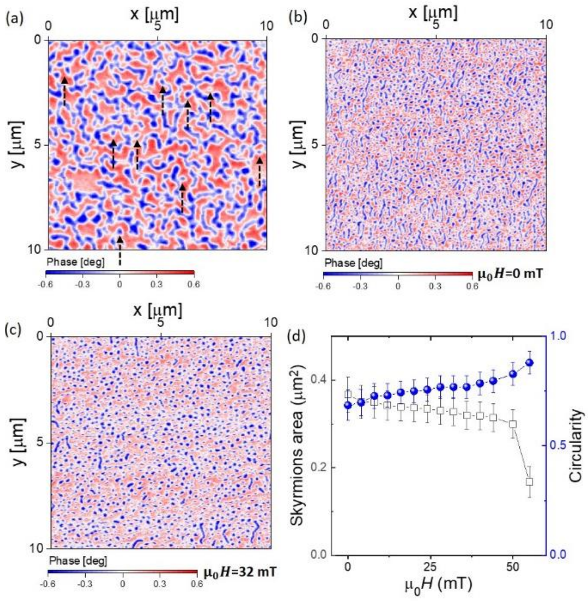

Fig. 7: MFM measurements on [Ir/Co(t_{Co})/Pt]$_5$ multilayers for t_{Co}=0.8nm at room temperature. (a) The MFM images were acquired in the as-grown state. Red and blue contrast represent the out-of-plane magnetizations of opposite direction. Some skyrmions are indicated by dashed black arrows. (b) As grown-state modified by the “in-plane field procedure”. (c) An example of the evolution of skyrmions vs the perpendicular applied magnetic field for $\mu_0 H = 32\mathrm{mT}$. (h) A plot showing the area of the skyrmions (open square) and circularity (blue spheres) vs $\mu_0 H$.

For further information on this topic contact Murat Cubukcu (murat.cubukcu@npl.co.uk), Olga Kazakova (olga.kazakova@npl.co.uk).

4.2.5 Thermoelectric Signature of Individual Skyrmions

Skyrmions are nano-scale topologically non-trivial spin structures which are inherently robust due to their particular topology and can be driven efficiently by electrical currents. Their electrical characterization and manipulation have been investigated intensely over recent years. However, only very few studies have addressed their thermoelectrical properties.

Part of the work within this project involved investigation of the thermoelectric response skyrmions. Here, we studied the thermoelectrical signature of individual skyrmions in a Pt/Co/Ru multilayer microdevice using an all-electrical single-shot technique. We achieve this by employing a highly controlled nucleation process using nanosecond current pulses to nucleate single skyrmions. The skyrmions were confirmed by performing magnetic force microscopy (MFM) imaging of the microdevice. Subsequently, we controllably annihilate them using a novel approach employing a highly localized stray magnetic field provided by the MFM probe. We attribute the observed thermoelectric signature, unambiguously, to the resulting thermoelectric response to the anomalous Nernst effect (ANE) originating from the spin structure of the skyrmions. For the experimental conditions used in this work, we define a thermoelectric signature of 4.6 nV per skyrmion. Furthermore, the topological contribution to the Nernst signal that might arise due to presence of the skyrmions is discussed, see Fig. 8.

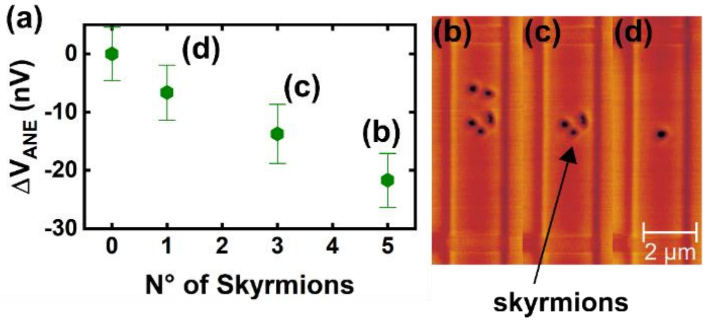

Fig. 8: (a) ANE voltage, V_ANE, as a function of the skyrmions present in the microdevice. (b)-(d) MFM measurements sequences showing the skyrmion annihilation process. The green dots in (a) correspond to the skyrmion configuration in (b)-(d).

Our findings enable the unique non-invasive characterization, detection and counting of skyrmions in magnetic microdevices adding to the plethora of techniques available and present a route for spin caloritronic devices based on skyrmions. Furthermore, our work provides fundamental insight into the thermo-electrical properties of topological spin structures.

For further information on this topic contact Alexander Fernandez-Scarioni (alexander.fernandez-scarioni@ptb.de) and see https://doi.org/10.1103/PhysRevLett.126.077202.

4.2.6 Local Thermoelectric Response from a Single Néel Domain Wall

Part of the work **within this objective** involves local thermoelectric response from spin textures in confined nanometric structures. In this work, we demonstrate how a highly localised heat source, provide by a heated scanning probe, can generate a unique thermoelectric signature from a trapped domain wall, see Fig. 9(a). We show that this method is sensitive to the nanoscale spin texture of the domain wall, which allows us to extract the domain wall type. We find that the resulting thermoelectric response in our system is explicitly that of a Néel domain wall. This work represents the latest advancement towards the limits of understanding and the next logical step in thermoelectric imaging of nanoscale magnetic phenomena.

Over the past six years [*Bartell et al Nat. Commun. (2015)*] the relatively new field of spatially resolved thermoelectric detection has gained significant traction due to its applicability to areas such as spintronics and spin caloritronics. Here, the localised response offers a deeper insight over traditional thermoelectric methodologies that record the global response of the material system. This is particularly apparent in investigating domain configurations in antiferromagnetic systems [*Mei et al Adv. Mater. (2020), Janda et al Phys. Rev. Materials (2020)*], ultra-thin ferromagnets [*Pfitzner et al, AIP Adv. (2017), Iguchi et al. Sci. Rep (2020)*], and ferrimagnets (*Daimon et al Nat. Commun. (2016)*). These materials offer a rich plethora of characteristics that are exploitable for emerging spintronic technologies, including no or minimal stray fields, fast (THz) spin dynamics and current tunability. However, imaging the magnetisation structure of these materials at the nanoscale proves challenging and is typically limited to central facilities, such as X-ray magnetic linear/circular dichroism and/or photoemission electron microscopy. Thermoelectric imaging can circumvent this bottleneck, allowing greater freedom over the type of samples required, with the additional advantage of being performed in a laboratory setting.

Whilst significant progress has been made advancing the technique and exploiting its use for fundamental research, the authors are not aware of any studies that push the fundamental understanding of the thermoelectric response from domain walls. This is typically due to limited spatial resolution or low signal-to-noise. This is exemplified by recent published works which focus primarily on single shot measurements, imaging single magnetic domains (quasi static and time domain), or measurements at magnetic saturation. Therefore, explanations of the results are limited to a simple description of the local magnetisation within the magnetic domains, and the transition regions are usually unaddressed.

Using a heated scanning probe as the localised heat-source instead of a raster-scanned focused laser greatly improves the spatial resolution and sensitivity of the technique. We show that this leads to unambiguous detection of the thermoelectric signature of the domain wall for the first time, see Fig. 9(b). This enabled a more rigorous analysis of the discrete thermoelectric signals by analytical and micromagnetic models that better describes the complex interplay of magnetic and thermal phenomena.

The ability to discern the spin texture in domain walls or skyrmions, in a laboratory environment, is an invaluable step towards rapid prototyping of these textures in real world spintronics and spin caloritronic applications. This is especially true when one considers that domain walls and skyrmions based applications are steadily increasing in technological readiness.

For further information on this topic contact Craig Barton (craig.barton@npl.uk).

4.2.7 Diameter-independent skyrmion Hall angle observed in chiral magnetic multilayers

The topology of magnetic skyrmions, which originates in their chiral domain wall winding, governs their unique response to a motion-inducing force. When subjected to an electrical current that applies such a force by means of a spin-orbit torque, the chiral winding of the spin texture leads to a deflection of the skyrmion trajectory so that they travel at an angle, known as the skyrmion Hall angle, to the driving force. This angle is predicted to depend on the diameter of the skyrmion by the well-established Thiele model, which treats the skyrmion as a rigid particle-like object moving in a flat energy landscape.

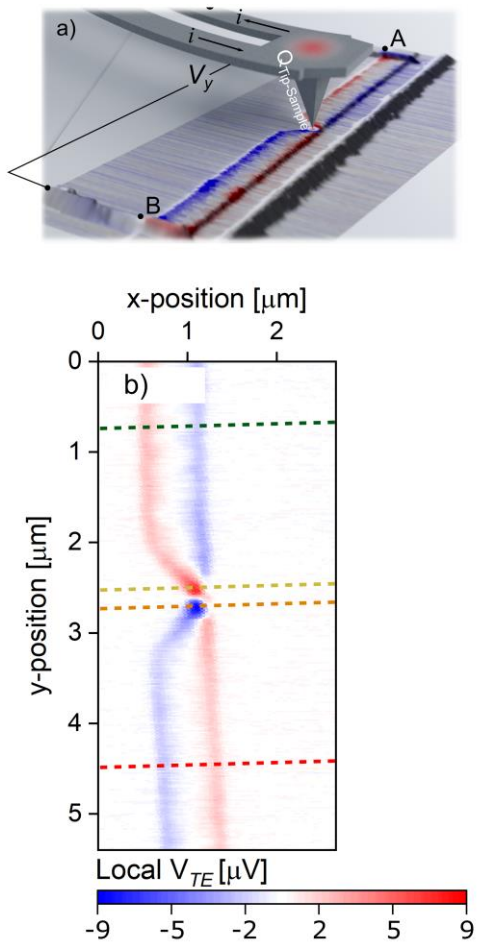

Fig. 9: (a) schematic overview of the experimental set-up for the local thermoelectric measurements showing the localised thermal heat source (heated AFM tip). (b) example thermoelectric data from a Néel domain wall.

We have studied skyrmions in Pt/CoB/Ir multilayers by means of scanning transmission x-ray microscopy at the PolLux beamline at the Swiss Light Source, see Fig. 10(a-b). A 2 µm wide magnetic wire was heated by means of a current pulse to nucleate skyrmions within it. Application of a field in the opposite direction to the magnetisation in the skyrmion core compresses the skyrmions, allowing the diameter to be varied. We then took snapshots of the magnetic textures within the wire after pairs of spin-orbit torque-inducing current pulses and tracked the changes in the position of each individual skyrmion after each pair. Examples of such tracks are given as series of coloured points in Fig. 10. By this means we could determine the average velocity and skyrmion Hall angle for each skyrmion of a known diameter, see Fig. 10(c-j).

In contrast to the Thiele model, our experimental study finds that the skyrmion Hall angle is diameter-independent for skyrmions with diameters ranging from 35 to 825 nm. At an average velocity of 6 ± 1 ms−1, the average skyrmion Hall angle was measured to be 9° ± 2°. In fact, the skyrmion dynamics is dominated by the local energy landscape such as materials defects and the local magnetic configuration.

For further information on this topic contact Christopher Marrows (C.H.Marrows@leeds.ac.uk) and see https://doi.org/10.1038/s41467-019-14232-9.

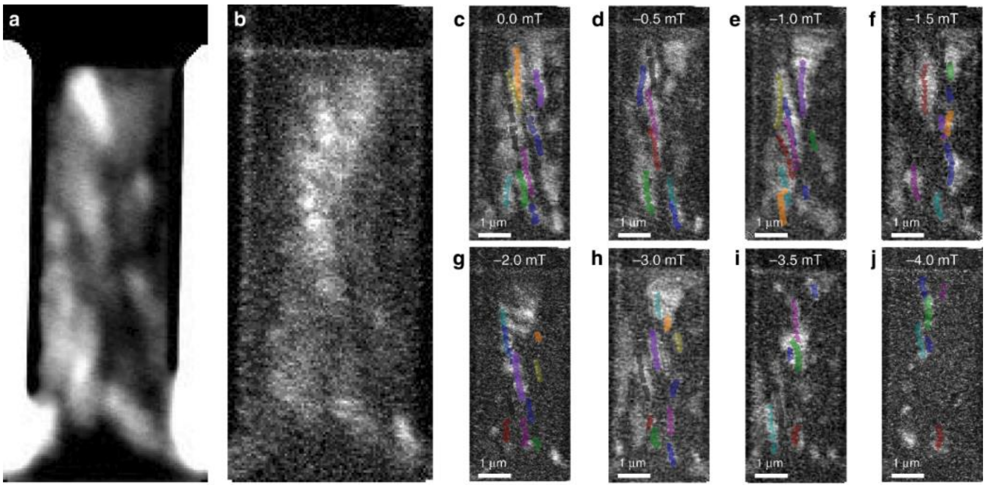

Fig. 10: a Average intensity map of all STXM images. Bright regions represent areas with high probability of containing a reversed magnetic domain or skyrmion. b Average intensity map of the absolute difference between consecutive images. Bright regions show high probability of an expanding magnetic domain or a moving skyrmion. c–j Average intensity map of the absolute difference between consecutive images obtained at each applied field, superimposed are the skyrmion centre positions (coloured symbols) throughout all the pulse series measured in this experiment.

4.2.8 Local manipulation of skyrmions using magnetic force microscopy

To investigate skyrmions mobility in thin films, INRIM and NPL obtained multi-layered thin films from the Institut für Physik, Johannes Gutenberg-Universität (Mainz, Germany). The thin films where perpendicularly magnetised X/CoFeB/MgO multilayers, with X = W, Pt, or Ta. The main properties, and the Dzyaloshinskii-Moriya interaction (DMI) constant are summarized in Table 1, which were measured at Mainz using a vibrating sample magnetometer, and at NPL through domain wall width(Woo et al., 2016).

Multilayer	M_s (A/m)	K_{eff} (J/m^3)	$\lvert D\rvert$ (mJ/m^2)	$\lvert D_S\rvert$ (pJ/m)
Si/SiO2/[Ta(5)/$Co_{20}Fe_{60}B_{20}$(1)/MgO(2)]15/Ta(5)	1.00 x10^6	4.6 x 10^5	0.08 ± 0.03	0.008 ±0.03
Si/SiO2/[W(5)/$Co_{20}Fe_{60}B_{20}$(0.6)/MgO(2)]15/Ta(5)	1.17 x10^6	4.1 x 10^5	0.61 ± 0.03	0.37 ±0.02
Si/SiO2/Ta(5.7)/[Pt(3.4)/$Co_{60}Fe_{20}B_{20}$(0.8)/MgO(1.4)]15/Ta(5).	1.54 x10^6	2.9 x 10^5	1.0 ± 0.1	0.080 ±0.08

Table 1. DMI values for the investigated films. The layer thickness in nm is indicated in brackets. Each film had 15 repetitions of the magnetically coupled layers.

Experiments were carried out to manipulate the magnetic domains in the thin films using a magnetic force microscope (MFM) to: (i) demonstrate how to nucleate and move skyrmions; (ii) generate skyrmions-to-skyrmion collisions to study pinning defects; (iii) demonstrate how to differentiate between probe-to-skyrmion and skyrmions-to-skyrmion interaction.

The MFM protocol consisted in: (1) Saturate the films with in-plane magnetic field(Zhang et al., 2018); (2) at zero field, image the topography of the surface using; (3) lift the MFM probe, ~100 nm, and apply a perpendicular field of ~65 mT; (4) image magnetization (i.e. MFM phase shift) in lift mode using topography recorded in a previous step; (5) To modify the magnetization of an area, scan with the probe in close proximity to the surface over that area; (6) Alternate between steps (4) and (5) varying the area scanned in (5) to bring the probe closer to a structure of interest (e.g., a skyrmions).

Following the protocol described above, NPL performed a series of experiments where the MFM probe scanned at varying distances from skyrmions. The results of those experiments are summarized in Fig. 11(a), where the displacement of the skyrmions is plotted against the minimum distance between the probe and the skyrmions (measured before performing the “writing” procedure, i.e. step (5) of the protocol). It is possible to see in Fig. 11(a) that there is a minimum distance where the skyrmions start to move or where the probe is too far away, and that this distance depends on the direction used for writing. This asymmetry is due to the “sensing point” of the probe and the “writing points” being in different positions and in general, depending on the shape of the stray field of the MFM probe.

The straight lines in Fig. 11(a) represent the ideal behaviour, either skyrmions moving for as long as the probe is interacting with it (red line), or zero displacement because the probe is too far away (blue line). The area coloured around the lines is to indicate a 75 nm uncertainty area, estimated as the uncertainty in position of the skyrmions between two different MFM images. It is interesting to note that while most of the experiments carried out fall on, or close to, the ideal lines, there are several data points which fall outside. These points correspond to situations where either there was a skyrmions collision, or there was pinning.

For instance, Fig. 11(b) shows a collision (left to right are sequential frames). The skyrmions marked in blue is pushed with the probe and interacts with the skyrmions marked in yellow. It is possible to see in the corresponding graph (Fig. 11(iv)), that the blue skyrmions moved much less than expected, and the yellow skyrmions, which was too far away from the probe to move, shows some displacement.

As a conclusion, the work has led to the development of a new method to manipulate skyrmions, which can now be used to characterize skyrmions, or skyrmions-related phenomena, in thin films or nanostructures.

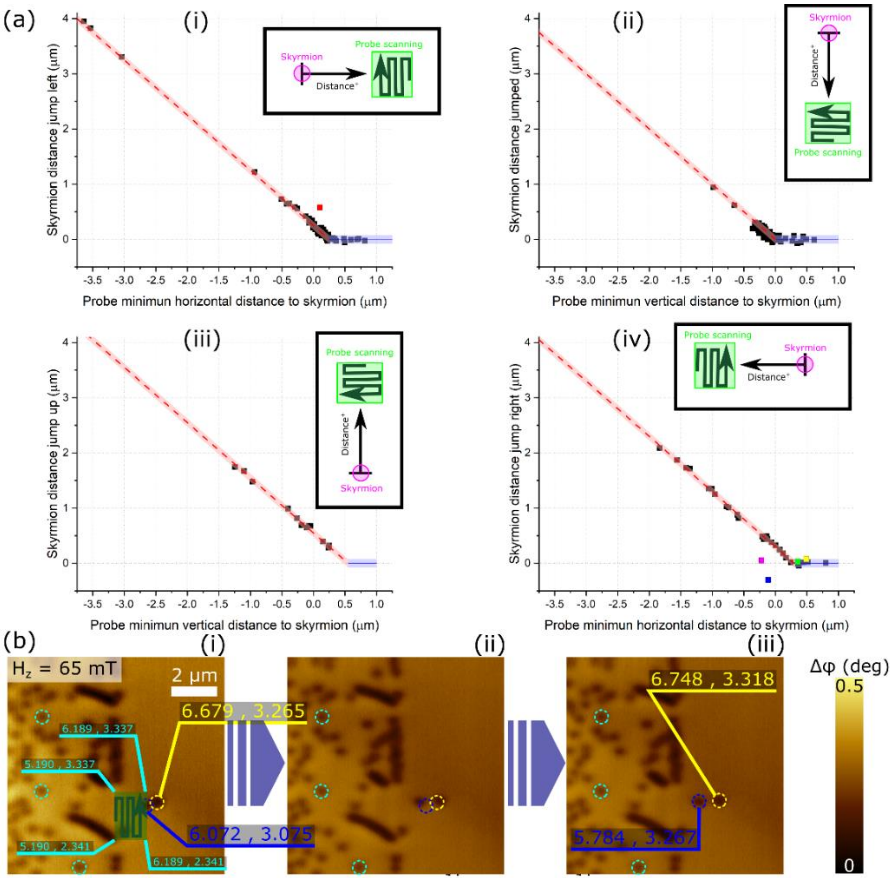

Fig. 11: Skyrmion manipulation using MFM probes. (a) Skyrmion displacement against probe-skyrmion distance. (i) to (iv) represent the four different directions used to move skyrmions. Insets indicate how positive and negative distance was defined, and from which direction the probe approximated to the skyrmions. (b) consecutive frames of skyrmions manipulation process. The green arrow indicates the area scanned by the probe between (i) and (ii). Coordinates are referred to the bottom left corner of the scanning area (cropped from the current image).

For further information on this topic contact Craig Barton (craig.barton@npl.co.uk) and see https://doi.org/10.1038/nmat4593, https://doi.org/10.1038/s42005-018-0040-5.

4.2.9. Key Outputs and Conclusions

Magnetic force microscopy (MFM) is a widespread technique for imaging magnetic structures with a resolution of some 10 nm. MFM can be calibrated to obtain quantitative (qMFM) spatially resolved magnetization data in units of A/m by determining the calibrated point spread function of the instrument, its instrument calibration function (ICF), from a measurement of a well-known reference sample. The project partners have together with collaborators explored how a Ti/Pt/Co multilayer stack can be used as a suitable reference material (https://arxiv.org/abs/2201.09763). Additionally, the consortium has used qMFM to analyse the radial dependent phase response of skyrmions in chiral magnetic multilayers. A simple model has been developed that treats the skyrmion size and domain wall as independent parameters, from which one can easily explore the role of each on the calculated expected phase response of qMFM. The results highlight how qMFM can be used to shed light on the underlying magnetization structure of skyrmions, and for the numerical or micromagnetic simulations results validation. It is anticipated that this work will help to expedite the process to optimize the magnetic parameters used for modelling skyrmionic systems, accelerating the technological development of skyrmionic systems. A corresponding paper detailing these findings has been submitted to a peer-reviewed journal.

Moving from qMFM techniques to other methods, a paper on the identification of Neel and Bloch type skyrmions by Lorentz Transmission electron microscopy (LTEM) which details the procedure to identify the skyrmion size using this method has been published on the arXiv (https://arxiv.org/abs/2002.12469) and as a peer-reviewed paper in Ultramicroscopy.

Another work performed by project partners has been devoted to comparing the results of different experimental methods namely magnetic force microscopy (MFM) and LTEM on nominally identical samples grown in the same batch. Since MFM and LTEM measurements require different substrates (electron transparent membranes in the case of LTEM and standard Si substrates in the case of MFM), no exact consensus on the appearance of skyrmions in temperature and magnetic field phase space could be reached, probably due to different strain in the deposited films. The paper has been submitted to a peer-reviewed journal and uploaded to the arXiv (https://arxiv.org/abs/2111.12634).

In addition, a large variety of thermoelectric and transport measurements have been undertaken. From this work a paper on individual skyrmion manipulation by local magnetic field gradients has been published in Communication Physics (https://arxiv.org/abs/1903.00367). An additional paper on the thermoelectric signature of individual skyrmions has been published in Phsical Review Letters (https://arxiv.org/abs/2001.10251v3). Moreover, a manuscript on deterministic field-free skyrmion nucleation has been published in Nano Letters (https://arxiv.org/abs/1902.10435).

Finally, project partners, together with collaborators, studied skyrmions in Pt/CoB/Ir multilayers by means of scanning transmission x-ray microscopy at the Swiss Light Source at the Paul Scherrer Institute. By this means the average velocity and skyrmion Hall angle for each skyrmion of a known diameter could be determined. The work has been published in Nature Communications (https://doi.org/10.1038/s41467-019-14232-9).

Based on these results, this objective was successfully achieved.

4.3 Analysis of novel dynamical and quantisation effects in TSS (objective 3)

4.3.1 Ferromagnetic Resonance with Magnetic Phase Selectivity by Means of Resonant Elastic X-Ray Scattering on a Chiral Magnet

In skyrmion hosting bulk materials such as the common B20 materials (MnSi, FeCoSi, Cu_2OSeO_3) the dynamic excitations in the skyrmion phase are well known and can be detected e.g. using ferromagnetic resonance based techniques. Typically, the three lowest lying modes require moderate magnetic fields and are in the low GHz range. Their unambiguous identification usually relies on micromagnetic simulations. In this project, researchers from the Technical University of Munich and the University of Regensburg first used soft X-ray based scattering techniques to locate the skyrmion lattice in magnetic field and temperature space. In combination with GHz magnetic field excitations it is then possible to identify the normal modes of the skyrmion lattice in reciprocal space.

Cubic chiral magnets, such as Cu_2OSeO_3, exhibit a variety of noncollinear spin textures, including a trigonal lattice of spin whirls, the so-called skyrmions. Using magnetic resonant elastic x-ray scattering (REXS) on a crystalline Bragg peak and its magnetic satellites while exciting the sample with magnetic fields at gigahertz frequencies, we probe the ferromagnetic resonance (FMR) modes of these spin textures by means of the scattered intensity. Most notably, the three eigenmodes of the skyrmion lattice are detected with large sensitivity. As this novel technique, which we label REXS FMR, is carried out at distinct positions in reciprocal space, it allows us to distinguish contributions originating from different magnetic states, providing information on the precise character, weight, and mode mixing as a prerequisite of tailored excitations for applications.

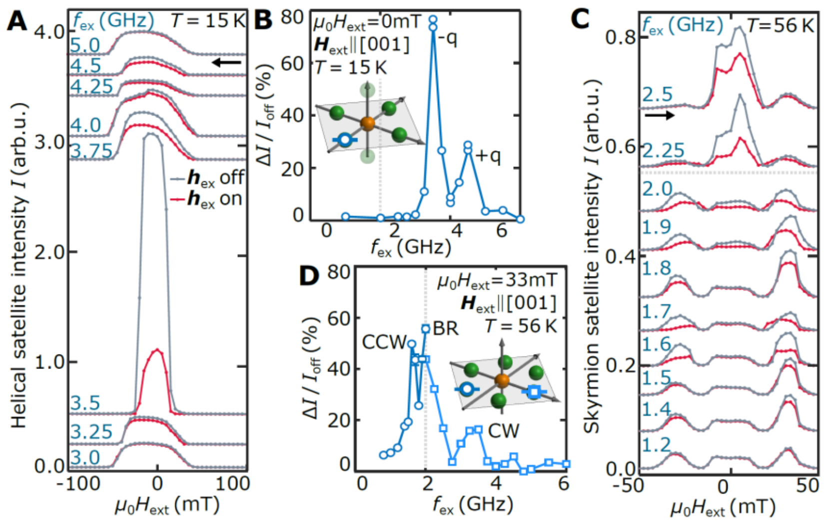

Fig. 12: REXS-FMR on the helical and skyrmion lattice phase of Cu_2OSeO_3. (A) Magnetic field scans at a helical reciprocal space location for different values of the excitation frequency f_{ex}. At each field step, data is recorded for inactive (gray curve) and active (red curve) excitation field. (B) Relative change of the helical spot intensity with applied excitation field at zero applied magnetic field. The inset shows the selected helical peak for the measurement. The two peaks correspond to the helical $+q$ and $-q$ modes. (C) Magnetic field scans at a skyrmion reciprocal space location for different excitation frequencies. The finite intensity around zero magnetic field arises from a helical reciprocal point that partly overlaps with the skyrmion one. (D) Relative reduction of the skyrmion peak intensity at $\mu_0 H_{ext}$ = 33 mT. The inset shows the skyrmion peaks used in the measurement. At the dashed line, the setup is modified de to re-adjustment and the measured skyrmion peak is changed slightly. Three maxima are observed that correspond to the counterclockwise (CCW), breathing (BR) and clockwise (CW) skyrmion modes.

For further information on this topic contact Christian Back (christian.back@tum.de) and see https://arxiv.org/abs/1909.08293.

4.3.2 Study of the Dzyaloshinskii-Moriya interaction and the perpendicular magnetic anisotropy at the $BaTiO_3$(BTO)/CoFeB interface

To date, most of the experimental works on interfacial Dzyaloshinskii-Moriya interaction (*i*-DMI) was focused on heavy metals/ferromagnet systems, where heavy metals was used to induce *i*-DMI. Recently, a sizeable *i*-DMI was observed to arise at the interface between an oxide layer and a ferromagnetic film. Due to the versatility of the oxide materials, featuring peculiar degrees of freedom, such as the terminations in a complex oxide and the polarization in a ferroelectric oxide, these systems are very promising for the design of layered structures with tailored *i*-DMI. In our work, published on Physical Review Letter, we performed a combined experimental and theoretical study of both the perpendicular magnetic anisotropy (PMA) and the *i*-DMI in the $BaTiO_3$(BTO)/CoFeB/Pt system, as a function of the oxide termination (TiO_2 vs BaO). The *i*-DMI was investigated by using Brillouin light scattering (BLS), measuring the frequency difference (Δf) between counter-propagating Damon-Eshbach (DE) spin-waves, induced by the presence of *i*-DMI, as function of the spin-wave wave vector k (Fig. 13). From linear fit to the experimental data, the effective DMI constant D was estimated to be 0.45±0.02 and 0.56±0.02 mJ/m^2, for TiO_2-BTO/CoFeB/Pt and BaO-BTO/CoFeB/Pt structures, respectively. Since the CoFeB/Pt interface gives the same contribution to the DMI of both systems, the different D values can be attributed to the influence of the oxide termination. The experimental results were interpreted by using first principles calculations. We found that *i*-DMI has an opposite sign at the BTO/CoFeB and CoFeB/Pt interface, therefore the total *i*-DMI of the system results from the competition of the two interface contributions. In particular, for both the BTO terminations the *i*-DMI has a negative sign indicating that the left-handed chirality is favored by the oxide layer. In addition, theoretical calculations showed that *i*-DMI strength at the TiO_2-BTO/CoFeB interface assumes a higher value than at BaO-BTO/CoFeB one in agreement with the experimental results. This finding was explained on the basis of the different electronic states around the Fermi level at the oxide/ferromagnetic metal interfaces and the different spin-flip process of the two terminations. On the contrary, PMA, investigated by superconducting quantum interference device magnetometry, was found to be larger for the CoFeB films grown on a BaO-BTO substrate.

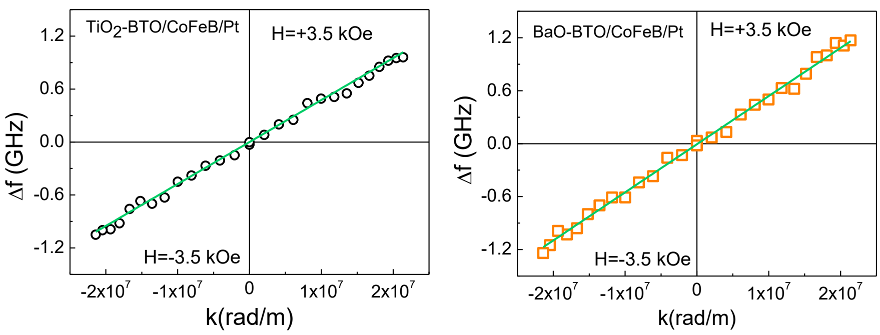

Fig. 13: Measured frequency asymmetry, Δf, as functions of **k** for CoFeB/Pt grown on TiO_2- (left panel) and BaO- (right panel) terminated BTO.

For further information on this topic contact Silvia Tacchi (tacchi@iom.cnr.it) and see https://arxiv.org/abs/2006.14268.

4.3.3 From propagative to stationary spin waves: suppression of the DMI-induced non-reciprocity by lateral confinement in magnetic dots.

Brillouin Light Scattering (BLS) experiments have been performed at Perugia University on samples consisting of Pt/CoFeB films grown at University of Mainz and patterned by e-beam lithography at PTB, in the framework of the TOPS project. In particular, the samples consist of bidimensional arrays of circular dots, patterned starting from a Pt/CoFeB bilayer, with a diameter d ranging from 100 nm to 400 nm, i.e., comparable with the wavelength of the thermal spin waves detected in BLS experiments. The aim of the experiments was to determine how the lateral confinement influences the spin-wave non-reciprocity induced by the presence of a sizeable interfacial Dzyaloshinskii-Moriya interaction (DMI) supplied by the heavy-metal substrate (Pt) on the ferromagnetic film (CoFeB). As illustrated in Fig. 14, the experimental results provide evidence for a strong suppression of the frequency asymmetry Δf between counter-propagating spin waves (corresponding to either Stokes or anti-Stokes peaks in BLS spectra), when the dot diameter is reduced from 400 nm to 100 nm, i.e. when it becomes lower that the wavelength of spin waves. Such an evolution reflects the modification of the spin-waves character from propagating to stationary and indicates that the method of quantifying the DMI strength from the frequency difference of counter-propagating spin waves is not applicable in the case of sufficiently small magnetic elements. Micromagnetic simulations are in progress at INRIM, using the MuMax^3 software package, to quantitatively reproduce the experimental results.

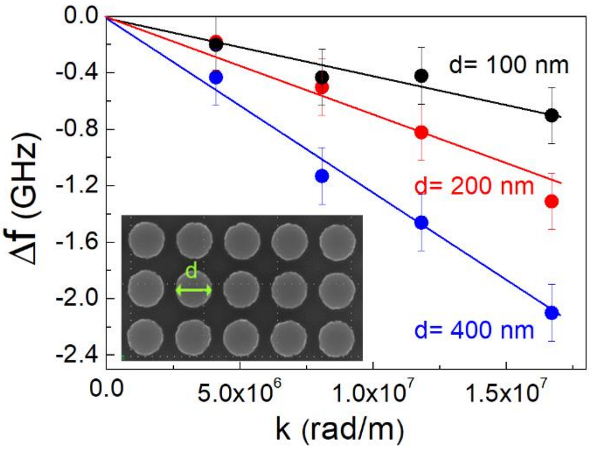

Fig. 14: Measured values of the frequency asymmetry Δf between Stokes and anti-Stokes peaks in Brillouin Light Scattering spectra measured on patterned arrays of circular magnetic Pt/CoFeB dots of diameter d=100 nm, 200 nm and 400 nm. It can be seen that the frequency asymmetry is strongly suppressed for d=100 nm, if compared to the case of d=400 nm.

For further information on this topic contact Giovanni Carlotti (giovanni.carlotti@unipg.it).

4.3.4 Tailoring interfacial effect in multilayers with Dzyaloshinskii-Moriya interaction by helium ion irradiation

In a recent paper published in Scientific Reports http://www.nature.com/articles/s41598-021-02902-y, we have demonstrated the control of the interfacial properties in Ta/[Pt/Co/Ta]$_{20}$ multilayers with Dzyaloshinskii-Moriya interaction (DMI) caused to the sample by the He^{+} irradiation (IR) using SQUID magnetometry, FMR and BLS. Our results show clear evidence of i) tailoring of interface ii) different magnetic properties in multilayers with different IR. As the IR increases, we observe that the perpendicular magnetic anisotropy (PMA) decreases significantly but after the IR reaches a certain level, it approaches saturation, while a reduction of the DMI is observed at intermediate IR which then stabilises at a constant value, slightly lower than the initial one, at high IR. The He^{+} irradiation induces short range atomic displacements, of the order of a few interatomic distances, leading to interface intermixing and hence altering the interface-driven PMA and DMI. He^{+} irradiation also shows a profound effect on the relaxation properties as demonstrated by a non-monotonic increase in damping value α. We see a correlation between resistivity and damping values. The results signify a large contribution of electron scattering on the relaxation properties He^{+} irradiated multilayers. Moreover, He^{+} irradiation can be used virtually in any kind of ultra-thin materials, including ferrimagnets and synthetic antiferromagnets. Finally, we should underline that we can control the magnetic properties of the thin films with DMI via He^{+} ion irradiation. This has consequences for the behaviour of skyrmions. For example, their nucleation, stabilisation, size, velocity and skyrmion Hall effect. The irradiation also opens up the possibility of new writing techniques which could be used to fabricate racetracks or logic devices without physically confining skyrmions via sample edges. Traditional lithographic techniques suffer from defects at boundary edges and skyrmions can be attracted to physical edges preventing efficient transport along the racetrack. This could provide a flexible way of designing countless possible structures for studying skyrmion behaviour or technological applications. The technique might be leveraged to generate a gradient of DMI, anisotropy or damping across the sample which could drive skyrmions from one side to the other with no external driving force, essentially creating a ramp for skyrmions.

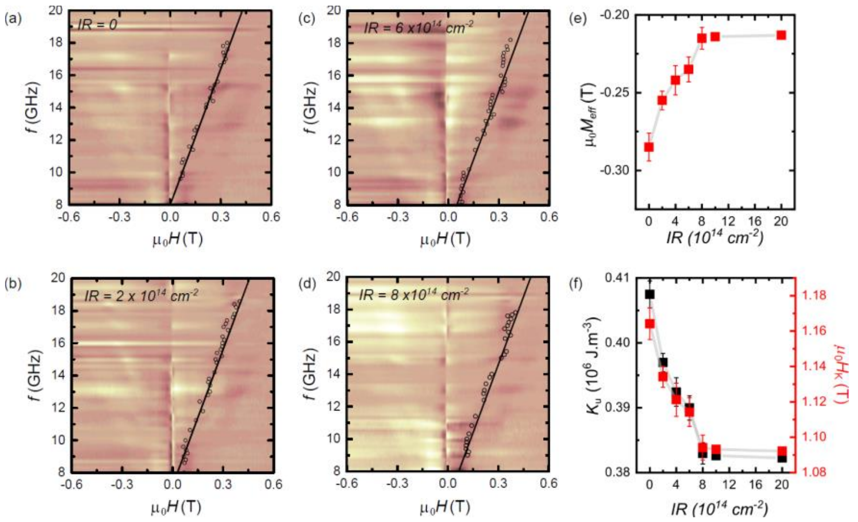

Fig. 15. (a-d) Microwave transmission as a function of frequency for different IR with the magnetic field perpendicular to the film plane. The black hollow markers depict the resonance field obtained by fitting FMR spectra and solid lines are fitting curve. (e-f) The effective magnetisation $\mu_0 M_{eff}$ (e) and the effective uniaxial anisotropy field $\mu_0 H_K$ (f) as a function of IR.

For further information on this topic contact Murat Cubukcu (murat.cubukcu@npl.co.uk), Olga Kazakova (olga.kazakova@npl.co.uk).

4.3.5 TR-MOKE studies of TSS

So far experimental studies of skyrmion eigenmodes mainly focused on the excitation by microwave magnetic fields and optomagnetical excitation using the inverse Faraday effect. These methods have in common that the dynamics are measured in thermodynamic equilibrium. Little is known on how the skyrmion dynamics change for resonant excitation of charge carriers, which is accompanied by ultrafast thermal gradients in time and space. Only one recently published study on a Néel-type skyrmion hosting material addresses this issue.

In our work we optically excite collective skyrmion eigenmodes in the chiral magnet $Fe_{0.75}Co_{0.25}Si$ and study their dynamics under a strong thermal gradient. The spin excitation is driven by a thermal modulation of magnetic anisotropy by laser heating and is probed by the time-resolved measurement of the magneto-optical Kerr effect (TR-MOKE) using laser pulses with 800 nm center wavelength and 150 fs pulse width. By making use of the cooling history dependence of $Fe_{1-x}Co_xSi$, we study the laser-induced spin dynamics not only in the skyrmion pocket, but also in the metastable skyrmion phase at lower temperatures.

In Fig. 16a the dynamics observed during a field cooling scan (FC+, compare with Fig. 16b) is shown. For the field-polarized and conical phase the observed dynamics are dominated by non-coherent processes, resulting from the laser-induced ultrafast de- and remagnetization. In comparison, for the metastable skyrmion phase we observe GHz oscillations, which are consistent with the breathing mode of the skyrmion lattice (Fig. 16c). These results demonstrate that collective skyrmion dynamics can be excited by the indirect coupling of the laser pulse with the spin system via laser heating in a non-equilibrium situation.

For further information on this topic contact Jantje Kalin (jantje.kalin@ptb.de).

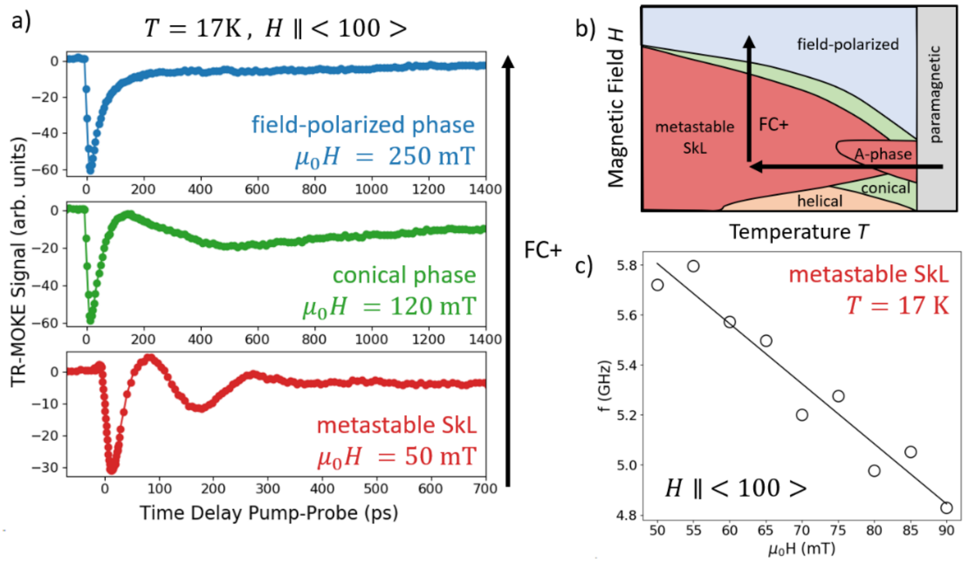

Fig. 16: a) TR-MOKE measurements of the field-polarized, conical and metastable skyrmion phase of $Fe_{0.75}Co_{0.25}Si$, b) Sketch of the magnetic phase diagram under field cooling through the skyrmion pocket (FC+), c) Oscillation frequency of the metastable skyrmion phase (SkL) versus magnetic field.

4.3.6 THz-spectroscopy of TSS

We fabricated a coplanar waveguide (CPW) with two squares of LT-GaAs to act as optical switches. The contacts were made from Ti/Au and in the centre of the central line of the CPW was a Hall bar made with a magnetic multilayer stack. A Hall bar was fabricated in the centre of the device via lithography and the magnetic material deposited by sputtering. The magnetic multilayers deposited included both ferromagnetic (FM) and synthetic antiferromagnetic (SAF) combinations based on CoB/Ir/Pt, with the ability to host skyrmions.

THz time domain spectroscopy (THz-TDS) measurements were performed using a Ti-Sapphire laser with 100 femtosecond pulses and central wavelength of 800 nm in a pump-probe arrangement. So far we have completed basic calibration and other tests to ensure the system works. We have measured the time delay vs. the current amplitude, see Fig. 17. From this, we took information about the pulse amplitude and width. Measurements were performed with different DC bias between -50 V and 50 V and different magnetic fields. A fast fourier transform of the pulse was also performed to reveal any absorbtion peaks. We have considered artefacts such as pulse reflections and have separated them from the main THz pulse and therefore improve the frequency resolution of the measurement. This work has been delayed by the COVID-pandemic and could not be fully finished.

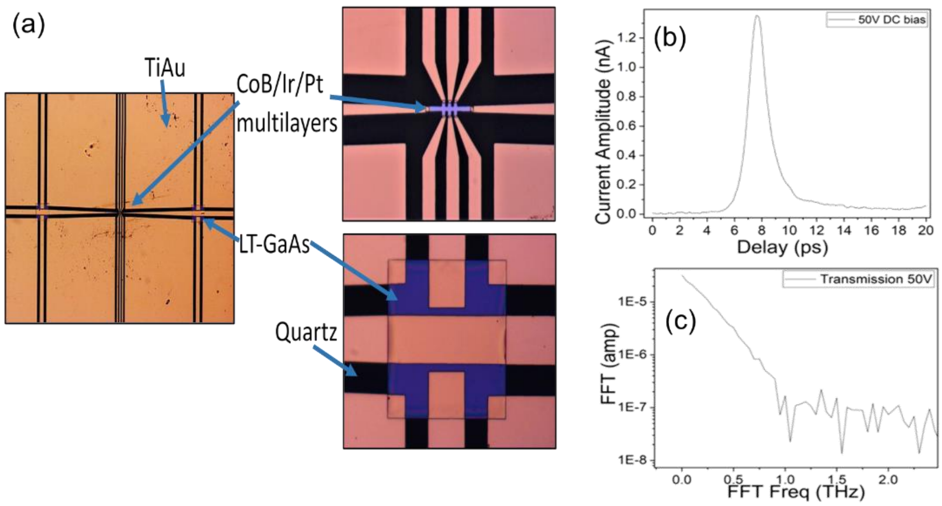

Fig. 17: (a) Photographs of the waveguide, (b) measured voltage pulse, (c) corresponding frequency spectrum.

For further information on this topic contact Bryan Hickey (B.J.Hickey@leeds.ac.uk).

4.3.7 Feasibility for new quantum standards

In a theoretical paper (https://doi.org/10.1103/PhysRevB.92.115417) Kamamoto et al. describe a hybrid system of a graphene monolayer coupled to a skyrmion crystal. They predict a topological quantum Hall effect which potentially could be used for novel electrical quantum standards operating at zero magnetic field. The experimental high-risk-high-gain research carried out with respect to this deliverable had the goal of studying and ideally verifying the predicted Hall quantization. However, the predicted quantization effect heavily relies on ultra-clean interfaces between the graphene monolayer and the topological spin structure (TSS). High quality epitaxial graphene mono- and bilayers were prepared at PTB by polymer assisted sublimation growth on SiC substrates. Unfortunately, despite of the high quality of the available graphene material it turned out that required excellent interface properties could not be achieved by placing the skyrmion hosting materials provided by TUM on top of the graphene layers. It became clear, that remaining impurities and particles between the two materials, the unevenness of the surfaces of the skyrmion hosting material, and the formation of non-magnetic layers on the surface of the skyrmion hosting material ultimately inhibit the formation of the required spin exchange coupling between to materials. Therefore, an alternative process was explored, where the hybrid material was inserted between the graphene and the substrate on which it was grown. This process allows one to realize ultra-clean hybrid bilayer systems consisting of graphene mono- and bilayers and ultra-thin metallic films. It is based on the intercalation of a few monolayers thin metallic film between the graphene and the SiC substrate. This process was demonstrated for the first time using liquid metal epitaxy of Ga at room temperature and ambient conditions. It allowed to reliably produce large area ultra-thin epitaxial Ga layers, also referred to as gallenene. The growth process of this hybrid material was studied in detail by x-ray photoelectron spectroscopy and Raman measurements, among others. The results revealed a promising alternative approach for the controlled fabrication of wafer-scale gallenene as well as for two-dimensional heterostructures and stacks based on the interaction between the liquid metal and the epitaxial graphene. Note that this heterostack consists of graphene, a material showing the quantum Hall Effect, and gallenene, a superconducting thin film. As such it might be suitable for integrated graphene quantum Hall arrays with superconducting leads. Furthermore, it is predicted to host topological edge states resulting from its honeycomb structure (https://doi.org/10.1088/2053-1583/ac0713) with further prospects for hybrid topologically protected quantum systems. The growth and structural properties of this novel hybrid material are discussed and reported in detail in the peer-reviewed publication, see https://arxiv.org/abs/1905.12438.

For further information on this topic contact Hans Werner Schumacher (hans.w.schumacher@ptb.de).

4.3.8. Key Outputs and Conclusions

Dynamic magnetoelectric modes in TSS have been extensively studied using ferromagnetic-resonance-(FMR)-based techniques and Brillouin light scattering (BLS). BLS measurements have been performed on He+ irradiated Co/Pt multilayers hosting skyrmions and the results have been compared to FMR measurements, achieving a careful determination of the first- and second- order anisotropy constants, as well as of the DMI constant, that are important parameters to tune the characteristics of skyrmion formation in these samples. The main results have been published in Scientific Reports (https://arxiv.org/abs/2105.03976).

Ferromagnetic resonance (FMR) studies have been performed for different alloys of FeCoSi as well as for Cu_2OSeO_3. These studies have been realized at different institutes and within a researcher mobility grant (RMG). Using X-ray magnetic circular-dichroism-based techniques (XFMR), the dynamic modes for Cu_2OSeO_3 have been unambiguously identified since this material showed the lowest damping parameter making the identification of the modes straight forward. The findings have been published in Physical Review Letters (https://arxiv.org/abs/1909.08293). Additionally, the identification of skyrmion modes in the low temperature skyrmion phase of the bulk B20 material Cu_2OSeO_3 has been achieved and published in Physical Review Letters (https://arxiv.org/abs/2011.07826).

Recently, it has been shown that certain materials possess a so-called metastable skyrmion phase (MSkL), where skyrmions exist in an extended parameter range. The project partners have studied the skyrmion dynamics in the MSkL for the first time. Using $Fe_{1-x}Co_xSi$ and employing time-resolved magneto-optical Kerr effect (TR-MOKE) measurements, the higher potential of the MSkL for applications as compared to the equilibrium skyrmion phase was demonstrated and it was shown that the MSkL is well suited to investigate generic properties of skyrmion dynamics. The studies have been summarized in a manuscript submitted for peer review and published on the arXiv (http://arxiv.org/abs/2202.04182).

Finally, some feasibility studies with respect to new quantum standards have been performed. The experimental high-risk-high-gain research carried out with respect to this deliverable had the goal of studying the predicted Hall quantization depending on ultra-clean interfaces between a graphene monolayer and a TSS. Unfortunately, despite of the high quality of the available graphene material it turned out that required excellent interface properties could not be achieved by placing the skyrmion hosting materials on top of the graphene layers. Instead, the project partners have studied an ultra-clean hybrid bilayer system consisting of graphene mono- and bilayers and ultra-thin metallic films. The growth and structural properties of this novel hybrid material are discussed in a paper published in Phys. Rev. Materials (https://arxiv.org/abs/1905.12438).

Based on these results, this objective was successfully achieved.

4.4 Protocols for reproducible growth of materials and reliable micromagnetic simulations and analytical tools (objective 4)

4.4.1 Growth of bulk TSS

Cu_2OSeO_3 in the $P2_13$ chiral cubic crystal structure the is one of the most important members of the chiral group. It was the first insulator in which the skyrmion lattice has been identified and it shows a magnetic B-T phase diagram which is very similar to the "generic" B-T phase diagram of other related members of this chiral group. In this material, recently, some new magnetic phases like the tilted conical spiral and the low-temperature skyrmion lattice phase as well as an elongated skyrmion phase have been observed. The insulating nature of this non collinear magnetic material makes the study of the decisive role of the crystal helicity interesting since in transport experiments using hybrid metal/magnet structures, the contributions due to conduction electrons in Cu_2OSeO_3 can be excluded.

We have grown Cu_2OSeO_3 single crystals using an optimized chemical vapor transport technique by using $SeCl_4$ as a transport agent. Single crystals of Cu_2OSeO_3 were grown by the standard chemical-vapor transport method. However, the novelty of this growth is the use of selenium tetrachloride ($SeCl_4$) as a transport agent. Previously, $SeCl_4$ has been mainly used to grow the molybdenum and tungsten diselenides.

Our optimized growth method allows to selectively produce large high quality single crystals. The method is shown to consistently produce Cu_2OSeO_3 crystals of maximum size 8 mm x 7 mm x 4 mm with a transport duration of around three weeks. We found this method, with $SeCl_4$ as transport agent, more efficient and simple compared to the commonly used growth techniques reported in literature with HCl gas as transport agent. The Cu_2OSeO_3 crystals have very high quality and the absolute structure is fully determined by simple single crystal x-ray diffraction. We observed both type of crystals with left- and right-handed chiralities. Our magnetization and ferromagnetic resonance data show the same magnetic phase diagram as reported earlier.

The crystal quality was examined with precision scans of XRD for full sphere approximation. The morphology and elemental analysis were examined using a Philips XL 30 scanning electron microscopy (SEM) equipped with a EDS system, which was operated at an accelerating voltage of 20 kV. The magnetization measurements were done using a Quantum Design MPMS-XL 7 SQUID magnetometer.

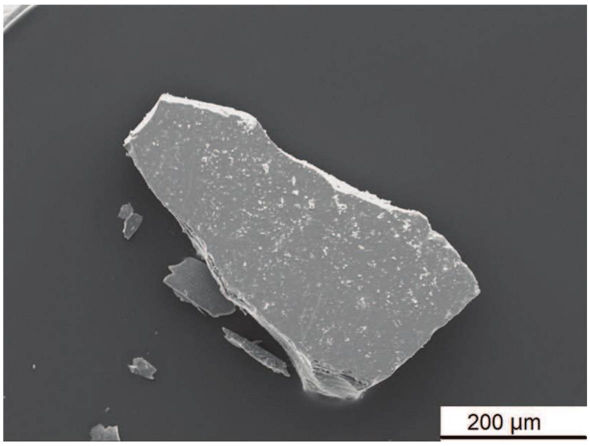

Fig. 18: Scanning electron microscopy image of a typical single crystal.

For further information on this topic contact Christian Back (christian.back@tum.de).

4.4.2 Growth of multilayer TSS

Magnetic multilayers that combine perpendicular magnetic anisotropy and a chiral Dzyaloshinkii-Moriya interaction are suitable for the observation of topological spin structures such as magnetic skyrmions and can easily be grown by magnetron sputtering. This growth process requires a vacuum chamber with a base pressure of the order of 10^{-8} mBar. In our chamber at Leeds an argon flow of around 63 sccm provides the necessary working gas pressure of 4-6 mTorr. Such multilayers can be grown on Si substrates, coated with a thermal oxide, at room temperature.

To give a representative example, the relevant metals were sputtered, sequentially, for known times using a recipe to produce magnetic multilayer with the following structure:

Ta(19s) | Pt(18s) | [CoB(15s) | Ir(5s) | Pt(9s) $]_{xN}$ | Pt(20s), (1)

where N is the number of repeats grown and the sputtering current and power used during growth are given in Table 2. The interfaces between the ferromagnet CoB and the heavy metals Pt and Ir provide the PMA and DMI.

Target Material	Current (mA)	Power (W) (Typical for applied current)	Average Growth Rate (Å/s)
Ta	50	14	1.18
Pt	25	9	1.36
CoB	50	13	0.51
Ir	25	9	3.00

Table 2: Typical growth conditions for magnetic multilayer growth using DC magnetron sputtering.

The growth rates shown in Table 1 were determined using the total growth times for the multilayer in combination with an x-ray reflectivity (XRR) measurement of either the original or sister (grown on the same sample plate) samples.

Figure 19 shows an example of a typical XRR measurement for a multilayer with the structure given in (1) where N=3. A simulation, performed using the GenX software [Björck and Andersson, J. Appl. Cryst. 40, 1174 (2007)], has been fitted to the XRR data, using a structure of:

Ta(22.5 Å)|Ta_2O_5(3 Å)|Pt(25 Å)|[CoB(7.7 Å)|Ir(15.0 Å)|Pt(9.2 Å)$]_{x3}$|Pt(29.6 Å). (2)

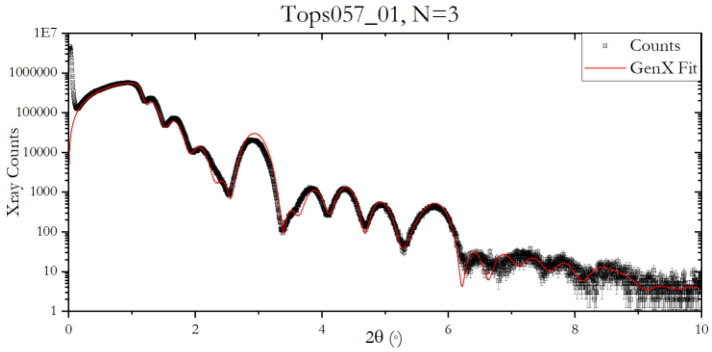

Fig. 19: The raw XRR data for example sample, Tops057_01, plotted with the final GenX fit from simulating the layer.

For further information on this topic contact Christopher Marrows (C.H.Marrows@leeds.ac.uk).

4.4.3 DMI quantification in magnonic crystals and isolated nanostructures

In the framework of the TOPS project, researcher operating at Perugia University, in collaboration with colleagues at INRIM-Torino, exploited virtual experiments based on micromagnetic simulations to show that the effect of DMI can be quantified not only in the case of plane films, but also for magnonic crystals consisting, for example, of arrays of interacting Permalloy nanowires deposited over a plane film. In particular, the results of a systematic micromagnetic study, using the GPU-accelerated software MuMax3, of the effect of DMI on the spin wave band structure of two one-dimensional magnonic crystals (MCs), both with the same periodicity p=300 nm, but different implementation of the DMI modulation have been presented at JEMS-2020 conference and just published in the Journal of Magnetism and Magnetic Materials (https://arxiv.org/abs/2112.05360). In a first system (Sample A) the artificial periodicity was achieved by modulating the interfacial DMI constant D, while in the second system (Sample B) also the sample morphology was modulated. Due to the folding property of the band structure in the dispersion relations of the magnonic crystals it is possible to extend the sensitivity of Brillouin light scattering towards weak DMI strength (D in the range from *0* to 0.5 mJ/m^2), by measuring the frequency splitting of folded modes in high-order artificial Brillouin zones, since the splitting increases almost linearly with the band index, as shown in Fig. 20. For relatively large values of the DMI (D in the range from *1.0* to *2.0* mJ/m^2), instead, the spin waves dispersion relations present flat modes for positive wavevectors, separated by forbidden frequency gaps whose amplitude depend on the value of D. These frequency gaps are more pronounced for the sample with morphology modulation.

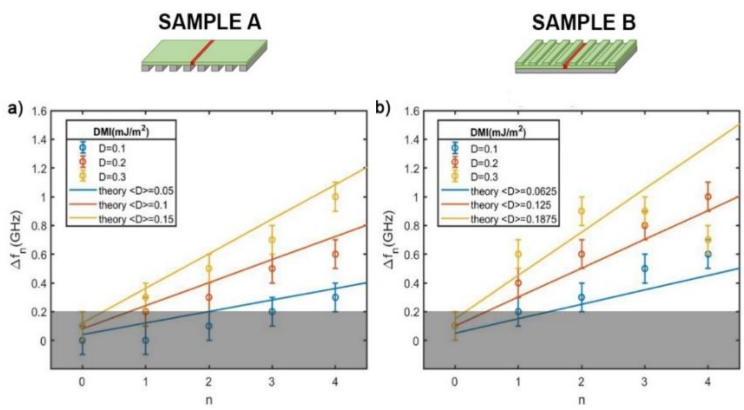

Fig. 20 Frequency asymmetry of spin waves with discrete wavevectors ± k_n (that can be obtained summing or subtracting to the spin wave wavevector ±k_0 an integer number n of grating wavevectors $k_G=2\pi/p$) for relatively small value of D in sample A (a) and in sample B (b). The points are results of the micromagnetic simulations, while the lines are obtained from the theoretical formula valid for a plain film, assuming an average value of D. From (https://arxiv.org/abs/2112.05360.

In a second study, just published on Applied Sciences https://doi.org/10.3390/app11072929, the characteristics of spin waves eigenmodes in isolated magnetic nanostructures, such as elliptical dots magnetized in-plane, with lateral dimensions of the order of 100 nm, were analyzed by micromagnetic simulations in presence of a sizeable DMI. It was shown that the eigenmodes spectrum is appreciably modified by the DMI-induced non-reciprocity in spin-waves propagation: the frequencies of the eigenmodes are red-shifted and their spatial profiles appreciable altered due to the lack of stationary character in the direction orthogonal to the magnetization direction, as shown in Fig. 21. As a consequence, one finds a modification of the expected cross-section of the different modes in either ferromagnetic resonance or Brillouin light scattering experiments, enabling one to detect modes that would remain invisible without DMI. In this respect, the modifications of the spectrum can be directly connected to a quantitative estimation of the DMI constant. Moreover, it is seen that for sufficiently large values of the DMI constant, the low-frequency odd eigenmode changes its profile and becomes soft, reflecting the transition of the ground state from uniform to chiral.

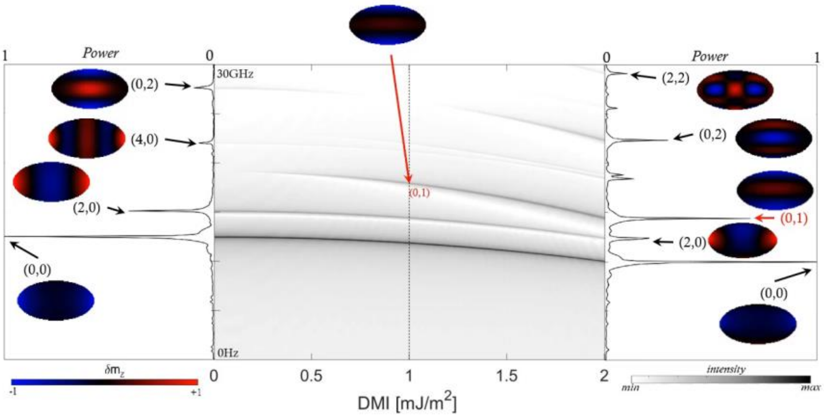

Fig. 21 Dependence of the frequencies of the spin wave eigenmodes on the DMI constant *D* for the elliptical dot of lateral dimensions *100×50 nm^2*. On the left- and right-hand sides, the intensity spectra corresponding to *D* = 0 and *2 mJ/m^2* are reported, respectively, together with the color insets that represent the spatial profile of the dynamical magnetization, expressed as the product of the modulus of the dynamical magnetization by the sign of its phase. From https://doi.org/10.3390/app11072929.

For further information on this topic contact Giovanni Carlotti (giovanni.carlotti@unipg.it).

4.4.4 Influence of the interfacial Dzyaloshinskii-Moriya interaction on the band structure of one-dimensional magnonic crystals

Researchers operating at Perugia University have investigated the effect of periodic interfacial Dzyaloshinskii-Moriya interaction on the spin wave (SW) dispersion relation of one-dimensional magnonic crystals (MCs). MCs consist of an extended CoFeB film, 1 nm thick, sitting over an array of Pt stripes having a thickness of 7 nm. Two set of samples having a periodicity of the Pt stripes p=400 nm (with a stripe width w=200 nm) and p=200 nm (with a stripe width in the range between 150 and 170 nm) have been studied. SW dispersion was measured by Brillouin light scattering in the Damon-Eshbach geometry, applying the external magnetic field along the stripe axis and sweeping the in-plane transferred wave-vector (k_z) along the perpendicular direction. The experimental results have been compared to the band diagram calculated by means of the plane wave method. In agreement with theoretical calculations, in all the investigated samples we observe the presence of low-frequency flat bands, due to appearance of SW modes localized in the areas where the Pt stripes are present. The frequency position of the flat band is found to strongly depend on the stripes period. Moreover, for the samples having smaller periodicity the dispersion curves are characterized by a marked qualitative change. In particular, we find SWs modes, featuring a strong non-reciprocal intensity, which are present in the SW dispersion only for positive wavevectors.

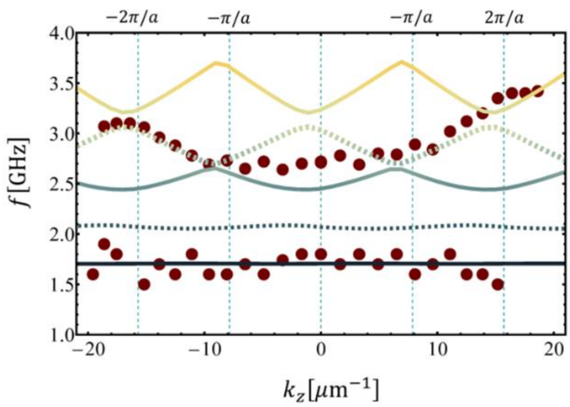

Fig. 22: Measured (points) and calculated (lines) SW dispersion relation of the sample having a periodicity of the Pt stripes p=400 nm and a stripe width w=200 nm.

For further information on this topic contact Silvia Tacchi (tacchi@iom.cnr.it).

4.4.5 Dynamical eigenmodes of Néel Skyrmions: from isolated elements to a one-dimensional magnonic crystal

In the framework of the TOPS project, researcher operating at Perugia University, in collaboration with colleagues at INRIM-Torino, exploited the micromagnetic software MuMax^3 to calculate the ground state and the dynamics of Néel skyrmions (SKs) in the range between 1 GHz and 30 GHz, in systems with three different levels of complexity, considering first the eigenmodes of an isolated SK, then the case of two interacting SKs and finally a linear chain of 71 units. For each simulation, the sample was discretized in cubic cells of side 1 nm and the spin-wave eigenmodes, excited by a pulse of external magnetic field, have been studied as a function of the intensity of the Dzyaloshinskii-Moriya (DMI) constant D and the exchange constant A. It has been shown that the band structure of one-dimensional magnonic crystals consisting of interacting Néel SKs can be interpreted in terms of magnonic bands that derive from the main eigenmodes of isolated SK, separated by forbidden band gaps. However, this simple picture is a good approximation only for either relatively small values of the DMI constant D or for relatively large values of the exchange constant A. In general, instead, the magnonic band structure is characterized by hybrid collective excitations, with anticrossing and band repulsion phenomena, caused by the dipolar interaction among the elemental constituents of the chain. Consequently, the amplitude of the permitted frequency bands and of the forbidden gaps are remarkably sensitive to variations of both D and A in the range of values typical of current ferromagnetic materials. This suggests that both parameters could be in principle exploited for fine-tuning the permitted and forbidden operation frequencies of future devices based on such kind of skyrmionics magnonic crystals.

For further information on this topic contact Giovanni Carlotti (giovanni.carlotti@unipg.it) and see https://arxiv.org/abs/2112.04967.

4.4.6. Key Outputs and Conclusions

Protocols for reproducible growth of TSS have been developed. To this end, different growth parameters have been optimised with the aim of obtaining stable high-quality thin-film materials and large-size high-quality bulk materials. The size aspect is especially important for future applications since at present the bulk material size is restricted a few millimetres. In total, a variety of multilayer and bulk samples have been grown and characterised. Samples have been shipped to partners for further experiments completing this task successfully.

Despite previous theoretical work, the development of new models was an essential prerequisite to validate the experimental results obtained in this project. Several phenomena such as the anomalous Hall effect, magnetoelectric modes, and spin-charge coupling could only be reliably interpreted and assigned to TSS characteristics with the availability of accurate simulations. To this end the project partners performed joint micromagnetic simulations.

A first study concentrated on the spin wave eigenmodes of isolated elliptical nanodots, showing the effect of DMI on both the eigenmodes frequencies and their spatial character. The results have been published Appl. Sci. (https://doi.org/10.3390/app11072929).

A second micromagnetic study was concerned with magnonic crystals consisting of a ferromagnetic film supported by an array of heavy-metal stripes. The effect of DMI on the magnonic bands of the magnonic crystal was investigated, suggesting a way to take advantage from the artificial periodicity of the magnonic crystal to achieve a better sensitivity in the determination of the DMI constant by BLS. The work has been published in the Journal of Magnetism and Magnetic Materials (https://arxiv.org/abs/2112.05360).

A third micromagnetic analysis concentrated on the eigenmodes of single and coupled skyrmions, showing that the band structure of a chain of skyrmions can be interpreted starting from the eigenmodes of a single isolated skyrmion and then considering the effects of both dipolar and exchange coupling. The work has been published in published in IEEE Magn. Lett. (https://arxiv.org/abs/2112.04967).

Finally, the project partners have employed a non-abelian gauge theory to derive the relation between the potential form of the magnetic DMI energy term. The key outcome of the theory is that the traditional spatial derivative appearing in the micromagnetic energy functional, must be substitution by a gauge covariant derivative which includes a gauge field. This theory has implications for determining surface-DMI and bulk-DMI terms.

Based on these results, this objective was successfully achieved.

5 Impact

This project has created impact for the scientific, metrological, industrial and end user communities through fundamental investigations on spintronics of magnetic nanolayers and nanosystems with the first steps towards traceable measurements on such devices, initial research towards future metrological applications, and availability of a good practice guide for accurate characterisation of topological spin structures. The latter will form the basis for a possible future measurement service in Europe.

Key dissemination activities to date are (i) 71 presentations at international conferences such as MMM-Intermag, CLEO, CPEM, JEMS, or SPIE Photonics West; (ii) 22 published articles in peer-reviewed journals such as Nano Letters, Communication Physics, Physical Review Letters, Physical Review B, Applied Physical Letters; additionally, 4 papers have been submitted to peer-reviewed journals; (iii) four newsletters and several interactive training courses/talks accessible form the project webpage. These achievements outperform the initial targets, despite institute closures due to COVID-19.

Impact on industrial and other user communities

ICT is an important sector for economic development in Europe and affects economic growth across the economy. The research in this project has enabled a fundamental understanding of novel spintronic effects, possibly enabling promising new device concepts.

Close cooperation between NMIs and leading research institutes has provided unique expertise to support the existing research networks on topological spin structures in Europe. Such cooperation might also lead to a follow-on collaboration after the project lifetime and, thus, strengthen the research in Europe. European researchers pioneered this field and are at present among the leading experts. Moreover, several national programmes on topological spin structures are still running. Interaction with different national programmes was an important dissemination activity, e.g., through jointly organised workshops. The DMI already has an influence on today's magnetic nanoscale devices. With an ongoing decrease of the size of such devices, the influence will even become more important. The successful implementation of the project concerning a Round-Robin comparison and guidelines for accurate measurements of the DMI constant is an achievement from which industry will profit in the short- and long term, respectively.

The project yielded information about charge-spin coupling in TSS, single skyrmion detection, and dynamics of TSS. Such information will be essential for future applications of TSS, e.g., for racetrack memory devices, high density storage devices, or logic devices.

Impact on the metrology and scientific communities

The accuracy of the determination of the DMI strength is crucial for the design of future applications employing TSS, e.g., novel types of magnetic memories. Only if the DMI strength is uniquely defined and measured, a clear relation with intrinsic or extrinsic material properties can be established. This project has taken a major step to resolve this key scientific controversy by organising a round robin (RR) comparison measurement involving the world-leading groups in the field. For the first time the effects of different measurement setups on the determination of the DMI constant could be pinpointed. A good practice guide for the measurement of the DMI constant by Brillouin light scattering was written. Brillouin light scattering appears to be currently the more reliable one, having a straightforward analysis of the measured data, not depending on the sample material or quality. A discussion of the measurement uncertainties and sources for systematic errors are included in the report This guide will form the basis for a possible future measurement service for the DMI constant in Europe.

The TOPS consortium was co-organiser of the Skymag 2020 workshop, which was supposed to take place in Paris from 6-9 April 2020. Due to COVID restrictions, the workshop was postponed to April 2021 and held as an online event. Additionally, two partners of the consortium (Brian Hickey, ULE and Massimo Pasquale, INRIM) chaired a session at the Joint European Magnetic Symposia (JEMS, which took place in Lisbon in December 2020) with the title "Magnetic based metrology tools and techniques". This session included two talks from the TOPS consortium. A dissemination workshop had been held online together with the final meeting. During the dissemination workshop, Giovanni Finocchio from the University of Messina gave the plenary talk.

Impact on relevant standards

So far, no relevant standards exist related to the measurement of the DMI constant. The consortium was in regularly contact with IEC TC 113 and IEC TC 68 to explore the possibility of implementing an IEC standard. However, especially due to the DMI measurement comparison, it was shown that a standard would be too premature and additional studies and comparisons will be necessary before a new standard can be feasible.

Longer-term economic, social and environmental impacts

Several possible industrial products for TSS devices are currently envisaged in the scientific community. First, TSS allow for discrete magnetic states being of smaller size and energetically more stable than their single-domain counterparts. For this reason, it is envisaged that TSS may be used as bits to store information in future memory and logic devices, where the state of the bit is encoded by the existence or non-existence of the TSS. This will have significant economic impact since the global digital storage device market is anticipated to reach $ 6.27 billion by 2022. Second, the position of TSS within a nanostructure may be manipulated using low current densities. Thus, TSS also provides promising candidates for future racetrack-type storage or logic devices. Third, TSS exhibit strong gyrotropic and breathing modes at GHz frequencies, which might open the avenue for TSS-based microwave applications.

A major goal of the EU is a 20 % increase of energy efficiency and a corresponding reduction of CO_2 gas emissions by 2020. The use of low power magnetic logic and storage devices based on TSS could lead to more energy efficient ICT and CE devices enabling a significant reduction of global energy consumption.

Society needs technologies based on innovative and disruptive products and concepts. TSS offers the potential to create novel spin-based electronic devices with improved speed, reliability, and significantly decreased power consumption.

The research carried out in this project supports the above longer-term impacts.

6 List of publications

[1] S. Saha, M. Zelent, S. Finizio et al., “Formation of Néel-type skyrmions in an antidot lattice with perpendicular magnetic anisotropy”, Phys. Rev. B 100, 144435 (2019), https://arxiv.org/abs/1910.04515

[2] A. Casiraghi, H. Corte-León, M. Vafaee et al., “Individual skyrmion manipulation by local magnetic field gradients”, Commun Phys 2, 145 (2019), https://arxiv.org/abs/1903.00367

[3] S. Pöllath, A. Aqeel, A. Bauer et al., “Ferromagnetic resonance with magnetic phase selectivity by means of resonant elastic x-ray scattering on a chiral magnet”, Phys. Rev. Lett. 123, 167201 (2019), https://arxiv.org/abs/1909.08293

[4] K. Zeissler, S. Finizio, C. Barton et al., “Diameter-independent skyrmion Hall angle observed in chiral magnetic multilayers”, Nat Commun 11, 428 (2020), https://doi.org/10.1038/s41467-019-14232-9

[5] A. Fernández Scarioni, C. Barton, H. Corte-León et al., “Thermoelectric Signature of Individual Skyrmions”, Phys. Rev. Lett. 126, 077202 (2021), https://arxiv.org/abs/2001.10251v3

[6] G. Carlotti, “Pushing down the lateral dimension of single and coupled magnetic dots to the nanometric scale: Characteristics and evolution of the spin-wave eigenmodes”, Applied Physics Review 6, 031304 (2019), https://arxiv.org/abs/1908.11098

[7] Weinan Lin, Baishun Yang, Andy Paul Chen et al. “Perpendicular Magnetic Anisotropy and Dzyaloshinskii-Moriya Interaction at an Oxide/Ferromagnetic Metal Interface”, Phys. Rev. Lett. 124, 217202 (2020), https://arxiv.org/abs/2006.14268

[8] C. Back, G. Carlotti, A. Casiraghi et al., “Measuring Interfacial Dzyaloshinskii-Moriya Interaction: A Review”, Proceedings 26, 41 (2019), https://doi.org/10.3390/proceedings2019026041

[9] S. Finizio, K. Zeissler, S. Wintz et al., “Deterministic Field-Free Skyrmion Nucleation at a Nanoengineered Injector Device”, Nano Lett. 19, 7246-7255 (2019), https://arxiv.org/abs/1902.10435

[10] S. Pöllath, T. Lin, N. Lei et al., “Spin structure relation to phase contrast imaging of isolated magnetic Bloch and Néel skyrmions”, Ultramicroscopy 212, 112973 (2020), https://arxiv.org/abs/2002.12469

[11] A. Aqeel, J. Sahliger, T. Taniguchi et al., “Microwave spectroscopy of the low-temperature skyrmion state in Cu2OSeO3”, Phys. Rev. Lett. 126, 017202 (2021), https://arxiv.org/abs/2011.07826

[12] A. Sud, S. Tacchi, D. Sagkovits et al., “Tailoring interfacial effect in multilayers with Dzyaloshinskii–Moriya interaction by helium ion irradiation”, Sci. Rep. 11, 23626 (2021), https://doi.org/10.1038/s41598-021-02902-y

[13] S. Finizio, S. Wintz, S. Mayr et al., “Time-resolved visualization of the magnetization canting induced by field-like spin–orbit torques”, Appl. Phys. Lett. 117, 212404 (2020), https://doi.org/10.1063/5.0029816

[14] S. Finizio, S. Wintz, S. Mayr et al., “Current-induced dynamical tilting of chiral domain walls in curved microwires”, Appl. Phys. Lett. 116, 182404 (2020), https://doi.org/10.1063/5.0005186

[15] A. Magni, V. Basso, A. Sola et al., "Spin Hall Magnetoresistance and Spin–Orbit Torque Efficiency in Pt/FeCoB Bilayers," in IEEE Transactions on Magnetics 58, 4400205 (2022), https://doi.org/10.1109/TMAG.2021.3084866

[16] R. Silvani, M. Kuepferling, S. Tacchi et al., “Impact of the interfacial Dzyaloshinskii-Moriya interaction on the band structure of one-dimensional artificial magnonic crystals: A micromagnetic study”, Journal of Magnetism and Magnetic Materials 539, 168342 (2021), https://arxiv.org/abs/2112.05360

[17] R. Silvani, M. Alunni, S. Tacchi et al, “Effect of the Interfacial Dzyaloshinskii–Moriya Interaction on the Spin Waves Eigenmodes of Isolated Stripes and Dots Magnetized In-Plane: A Micromagnetic Study”, Appl. Sci. 11, 2929 (2021), https://doi.org/10.3390/app11072929

[18] K. Szulc, S. Mendisch, M. Mruczkiewicz et al., “Nonreciprocal spin-wave dynamics in Pt/Co/W/Co/Pt multilayers”, Phys. Rev. B 103, 134404 (2021), https://arxiv.org/abs/2112.11206

[19] M. Bassotti, R. Silvani, and G. Carlotti, "From the Spin Eigenmodes of Isolated Néel Skyrmions to the Magnonic Bands of Skyrmionic Crystals: A Micromagnetic Study as a Function of the Interfacial Dzyaloshinskii-Moriya Interaction and the Exchange Constants," IEEE Magnetics Letters 13, 6101505 (2022), https://arxiv.org/abs/2112.04967

[20] J. Chen, H. Yu, and G. Gubbiotti, “Unidirectional spin-wave propagation and devices”, Journal of Physics D: Applied Physics 55, 123001 (2022), https://doi.org/10.1088/1361-6463/ac31f4

[21] B. Sakar, S. Sievers, A. Fernandez Scarioni et al., “A Ti/Pt/Co Multilayer Stack for Transfer Function Based Magnetic Force Microscopy Calibrations”, Magnetochemistry 7, 78 (2021), https://arxiv.org/abs/2201.09763

[22] S. Wundrack, D. Momeni, W. Dempwolf et al., “Liquid metal intercalation of epitaxial graphene: Large-area gallenene layer fabrication through gallium self-propagation at ambient conditions”, Phys. Rev. Materials 5, 024006 (2021), https://arxiv.org/abs/1905.12438

This list is also available here: https://www.euramet.org/repository/research-publications-repository-link/

7 Contact details

Dr. Mark Bieler
Physikalisch-Technische Bundesanstalt
2.4 Quantum Electronics
Bundesallee 100
D-38116 Braunschweig
Germany

phone: +49-531-592-2400
email: mark.bieler@ptb.de